NASA TN D-1897

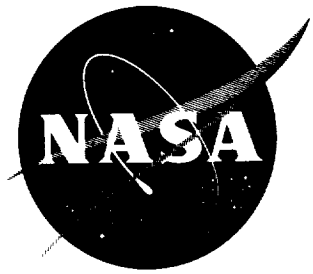

TECHNICAL NOTE

D-1897

EVALUATION OF A TECHNIQUE FOR DETERMINING TIME-INVARIANT AND TIME-VARIANT DYNAMIC CHARACTERISTICS OF HUMAN PILOTS

By Jerome I. Elkind, Edward A. Starr,
David M. Green, and D. Lucille Darley

Prepared under Contract No. NASw-185 by
BOLT BERANEK AND NEWMAN INC.
for
NATIONAL AERONAUTICS AND SPACE ADMINISTRATION
WASHINGTON
May 1963

Code-1

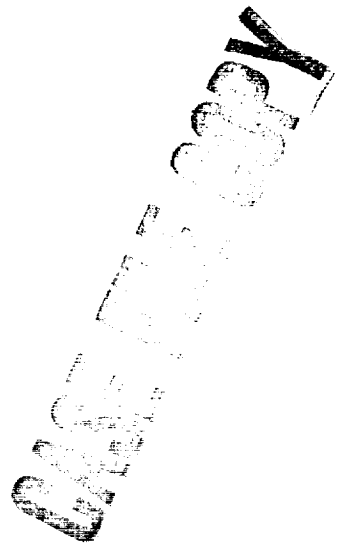

NATIONAL AERONAUTICS AND SPACE ADMINISTRATION

TECHNICAL NOTE D-1897

EVALUATION OF A TECHNIQUE FOR DETERMINING TIME-INVARIANT AND TIME-VARIANT DYNAMIC CHARACTERISTICS OF HUMAN PILOTS

By Jerome I. Elkind, Edward A. Starr,
David M. Green, and D. Lucille Darley

SUMMARY

A technique for determining the time-varying dynamic response characteristics of human pilots in tracking tasks is presented. The technique is based on a model adjustment or mimicking procedure in which a model composed of filters whose impulse responses are orthogonalized exponential functions is used. The filters are connected in parallel and their outputs are weighted and added together. The weights are determined so that the mean-square difference between the output of the model and the output of the pilot is minimum. Time-varying characteristics are measured by determining successively the model weights from short samples of the input and output signals of the human operator.

The model weights are partial regression coefficients of the pilot's output on each of the filter outputs used in the model. By making use of known statistical properties of regression coefficients, distribution functions for the model weights are derived for the case in which the residual error, the part of the pilot's output that cannot be accounted for by the model, has a normal distribution. Relations for estimating the length of sample of input and output signals required to determine the weights with given confidence limits are derived.

The measurement technique has been implemented on a high speed digital computer. Results obtained by applying the technique to measurement of a variety of digital filters, analog filters and human operator dynamic response characteristics are presented. It is shown that a model composed of five properly chosen filters can approximate a large variety of systems with an error of about one percent or less.

I. INTRODUCTION

The idea of representing human operator dynamic response characteristics by linear transfer functions so as to permit the application of the theory of linear servomechanisms to manual control problems originated during World War II in the work of A. Sobczyk, R. S. Phillips, and H. K. Weiss (refs. 1-3) and of Tustin (refs. 4-6). Tustin introduced the concept of determining (from measurements a human operator input and output) a linear operator to describe the human's dynamic characteristics and recognized the existence of a remnant, the portion of the human operator's response behavior that could not be attributed to this linear operation on the input. These early studies have served as the basis for much of research in human operator dynamic response characteristics that has been performed in the last fifteen years (see refs. 7 and 8 for a summary of this research).

An important aspect of research in human operator dynamics has been the development of techniques for determing human operator characteristics, that is, his transfer function. As might be expected from the fact that the human is an adaptive, time-varying, nonlinear controller whose characteristics depend upon the forcing function input to the control system and upon the characteristics of the controlled element, measurement of human operator dynamic characteristics presents some special problems. Frequently, it is not possible to remove him from the control system, to alter his connections with the rest of the system, or to apply special test signals as inputs without causing significant changes in his dynamic response behavior. Under these circumstances, it is necessary either to measure his characteristics in situ, that is, in the actual operational situation, or in a simulated situation in which the characteristics of those elements and signals which are important determinants of human operator behavior are faithfully reproduced (refs. 7-11).

Most measurements of human operator dynamic characteristics have been made using one of three techniques: Fourier analysis, correlation techniques, or model adjustment techniques. Tustin (ref. 6), Russell (ref. 10), and Sheridan (ref. 12), used input signals composed of a small number of sinusoids and performed a Fourier analysis of pilot output at each of the frequencies used in the input signal. Cross-correlation and cross-power density spectra techniques (refs. 13-15) have been used by Elkind (refs. 9,

16), Krendel (ref. 7) and Hall (ref. 11). Model adjustment techniques have been employed by a group at Goodyear Aircraft (ref. 17), Ornstein (ref 18), and Goodman and Reswick (ref. 19).

In the Fourier analysis technique an input forcing function composed of the sum of a small number of sinusoids is used. The correlation of the human operator's output with each of the sinusoids used in the input and by these sinusoids shifted in phase by 90 degrees is computed. The correlations obtained are the coefficients of the sine and cosine series representation of the part of the operator's response that is linearly related to the input. By normalizing these correlations with respect to the amplitudes of the input sinusoids, values of the human operator's transfer function are obtained at the frequencies contained in the input.

The correlation technique rests upon the fact that the cross-correlation function of input forcing function and human operator response is equal to the convolution of the input autocorrelation function and the impulse response of the linear operator that provides the least mean-square error approximation to the human operator's response. If the input is gaussian, the human operator's transfer function can be obtained by simply Fourier transforming the correlation functions. From the autocorrelation function of the human operator's response and its Fourier transform, the power spectrum of human operator's remnant can be determined. A modification of the correlation technique is to compute (1) the cross-power density spectrum between the input signal and the operator's response, (2) the power spectrum of the input and (3) the power spectrum of the response directly from the time functions of these signals without first computing the correlation functions. Human operator transfer function and the power spectrum of the remnant are determined directly from these power and cross-power density spectra.

In the third analysis method, the model adjustment technique, a model for the human operator is constructed and fed the same input as the operator. The parameters of the model are adjusted until a good match between model output and human operator output is achieved. A number of different model

matching techniques have been used. In the study conducted at Goodyear Aircraft (ref. 17), a model incorporating some simple nonlinearities was constructed on an analog computer. The parameters of the model, coefficients of the differential equation and of the nonlinearities that were simulated, were adjusted to obtain a good visual match to human operator's response. Ornstein (ref. 18) used an analog computer to simulate a linear model for the human operator. He automatically adjusted the parameters of the model (coefficients of a differential equation) to achieve the least mean-square error approximation to human operator characteristics. Goodman and Reswick (ref. 19) used what was essentially a tapped delay line (a delay-line synthesizer) to simulate the human operator's impulse response. The autocorrelation function of input signal to the operator (not the input forcing function to the system) was fed to the delay line. The outputs of the taps were weighted and then added together. The weights were adjusted to give a good visual fit to the cross-correlation function between input and response.

Each of these techniques has certain advantages and disadvantages. The Fourier analysis method is very simple and inexpensive to instrument and lends itself to real-time analysis of operator characteristics. The real and imaginary parts of the operator's transfer function can be computed as the tracking run is performed. However, the method cannot be used for determining the power spectrum of the remnant. Also, it is necessary to excite the system being studied artificially by a signal composed of sinusoids and therefore human operator characteristics cannot be measured using the signals naturally present in the system. Finally, samples of the system input and operator response signals must be several times longer than the period of the sinusoid at which measurements are being made or the sample length must be carefully adjusted to be an integral multiple of the periods of all the input sinusoids if accurate measurements are to be made. Sheridan (ref. 12) found that it was necessary to use samples 15 seconds long in order to obtain reasonably accurate transfer function measurements.

The correlation and spectral techniques have the advantage that the

power spectrum of the operator's remnant can be computed. However, the method is more complicated than the Fourier analysis technique and is not easily adapted to real-time, on-line data analysis. Artificial input signals must be used or it must be possible to isolate the input signal to the system. The sample length required to obtain accurate measurements depends upon the bandwidth of the filters used to find the power spectra. Typically, 25 to 30 second-long samples are necessary if reasonable resolution in frequency is to be achieved.

The model adjustment techniques permit measurement with the signals that normally circulate in the control loop and artificial inputs are not required. The principal advantage of the Goodyear and Ornstein techniques, which are based on simulation of a differential equation, is that they yield directly in closed form an analytic expression for the transfer function approximation to the human operator characteristics. However, the coefficients of this approximation, the coefficients of the differential equation, have to be determined by "cut-and-try" or "hill-climbing" procedures. There does not seem to be an analytic procedure for finding the coefficients. The technique also requires an assumption of the form of pilot transfer function. Since there may be a strong interaction among the coefficients being adjusted (the value of one coefficient influences the values of the others), inaccurate results may be obtained if the operator's actual characteristics are not of the assumed form. The remnant waveform can be determined by exciting the model with the input to the human operator and subtracting the model output from his output. The model adjustment technique of Goodman and Reswick does not require an assumption of the form of the human's characteristics. An analytic procedure for determining the weights that should be applied to the outputs of the tapped delay line exists (see ref. 20), although Goodman and Reswick used a "cut-and-try" procedure in their original work.

By taking advantage of some of the recent work on system analysis and signal representation, it seems possible to achieve considerable improvement in the accuracy of measurement of human operator characteristics and in the sample length required to obtain the estimates of his character-

istics. Levin, in his work on system analysis (ref. 20), points out that the model adjustment technique provides estimates of system characteristics that are optimum in the sense that they have minimum variance. Therefore, these estimates can be obtained with specified variance from shorter sample lengths than with less efficient techniques. His approach to the measurement problem is an application of the multiple regression analysis (refs. 21 and 22), and, as such, is an outgrowth of or is closely related to the work of Levinson (ref. 23), Goodman and Reswick (ref. 19), Lee (ref. 10), Gabor (ref. 24), and Knowles et. al. (ref. 25). Huggins in his work on signal representation (ref. 26) demonstrates the efficiency of representing a signal by orthonormal functions that resemble the signal to be represented. In particular, he shows that a particular class of orthogonalized exponential functions (ref. 27) are especially well suited for representing the impulse response of many physical systems. The techniques discussed in this report are a synthesis of the model adjustment (multiple regression) approach to measurement discussed by Levin and others and employs the orthogonal functions used by Huggins.

This research was supported by the National Aeronautics and Space Administration under contract NASw-185.

LIST OF SYMBOLS

a	Constant added to mimic to account for non-zero mean of $y(t)$
b_j	Mimic coefficient
$\underline{b}$	Vector of mimic coefficients
c_j	Coefficient of series representation of auto-correlation function $R_{xx}(t')$
C_{i1}, C_{i2}	Constants used to orthogonalize exponential functions
$e_i(t)$	Input forcing function signal
$F(s)$	Transfer function of test filter
g_j	The j^{th} element of g
$\underline{g}$	Second term of Eq. (3.15)
h	Digital sampling interval

h_j	The j^{th} element of $\underline{h}$
$\underline{h}$	Third term of Eq. (3.15)
$H(s)$	Human operator transfer function
K	Number of filters in mimic
K_ϵ	Error reduction factor
$\underline{L}$	Covariance matrix with elements $z_i z_j$
$\underline{L}_{K+1}$	Covariance matrix of z_i and z_j for $i \leq K$ and $j \geq K + 1$
m_j	Sample mean of $z_j(t)$
m_y	Sample mean of $y(t)$
$m(t-t')$	Weighting function of mimic
M	Number of degrees of freedom of z_{ju} in time T
$M(j\omega)$	Transfer function of mimic
$n(t)$	Noise signal representing pilot's remnant
n	Vector of covariances of $z_i(t)$ and $n(t)$
N	Number of independent samples of residual in time T
$R_{xx}(t')$	Autocorrelation of $x(t)$
s	Complex frequency variable $(\sigma + j\omega)$
s_h	Pole of system to be measured
$s_1, s_2, \ldots, s_K$	Poles of mimic filters
s_ϵ^2	Sample variance of residual
s_{ju}^2	Sample variance of part of output of j^{th} mimic filter that is uncorrelated with the other filter outputs
s_y^2	Sample variance of pilot output
$S_{xx}(j\omega)$	Power density spectrum of $x(t)$
$S_{yy}(j\omega)$	Power density spectrum of $y(t)$
$S_{\epsilon\epsilon}(j\omega)$	Power density spectrum of $\epsilon(t)$
t	Time
T	Length of sample of signals used to compute mimic coefficients
w_j	Coefficients of series expansion of system weighting function

$\underline{w}$	Vector of coefficients w_j for $j \leq K$
$\underline{w}_{K+1}$	Vector of weights w_j for $j > K + 1$
$w(t-t')$	Weighting function of time-invariant linear system
$w(t,t-t')$	Weighting function of time-variant linear filter
W_ϵ	Equivalent square bandwidth in cps of residual
W_{ju}	Equivalent square bandwidth of $z_{ju}(t)$
$W(s)$	Transfer function corresponding to $w(t)$
$x(t)$	Pilot visual input signal
$y(t)$	Pilot response signal
$\underline{Y}$	Vector of covariances of $z_i(t)$ and $y(t)$
$z(t)$	Mimic output
$z_j(t)$	Output signal of j^{th} mimic filter
ISE	Integral-square error
MSD	Mean-square difference
β_j	Expected value of b_j
$\underline{\beta}$	Vector of β_j
$\Delta\alpha$	Deviation of delay compensation from test filter delay
$\epsilon(t)$	Residual error signal
γ_j	Expected value of g_j
$\underline{\gamma}$	Vector of γ_j
$\sigma^2_{b_j\|s}$	Condition variance of b_j for a given s^2_{ju}
$\sigma^2_{b_j}$	Expected variance of b_j averaged over s^2_{ju}
σ^2_n	Variance of $n(t)$
σ^2_x	Variance of $x(t)$
σ^2_ϵ	Variance of residual
μ_y	Mean of $y(t)$
μ_j	Mean of $z_j(t)$
$\phi_j(t)$	Impulse response of j^{th} mimic filter
$\Phi_j(s)$	Transfer function of j^{th} mimic filter

II. THE MEASUREMENT PROBLEM

In Fig. 2.1 is a simplified block diagram of a flight control system. The pilot responds to the visual input signal, $x(t)$, by executing movements, $y(t)$, of the control. We are interested in the dynamic relationship between pilot response $y(t)$ and pilot input $x(t)$. Usually the input $x(t)$ is random or at least partly random. This is true even when the input forcing function is a fixed reference command, since, to a large extent, the signal $x(t)$ is composed of perturbations of electrical, mechanical or aerodynamic origin that circulate within the control loop.

Although the human pilot's characteristics are time-varying and nonlinear, we can always represent the relation between his input and his output in any control situation by the model of Fig. 2.2: a combination of a quasi-linear time-invariant or time-variant weighting function and a noise generator (refs. 7 and 9). The weighting function accounts for that portion of pilot output that is linearly correlated with the input. The noise generator accounts for that part not linearly correlated with the input, the remnant. For control situations in which the system dynamics or input forcing function do not change with time a time-invariant weighting function will frequently account for almost all of the pilot's response and the remnant will be small. When the system or input change with time, a time-variant weighting function is likely to be required to obtain a good representation for pilot behavior.

The weighting function is called quasi-linear because it approximates the relation between pilot input and output for only a single control situation. If the control situation changes (and sometimes even if it does not), a different weighting function will be required. The measurement problem is to determine the weighting function whose response to the pilot's input $x(t)$ provides the best match to the pilot's output $y(t)$. For the purposes of this report, we will consider the best match to be the one that causes the mean-square difference (MSD) between pilot output and weighting function response to be minimum. In addition to finding the weighting function, we want to determine the remnant $n(t)$. These are two elements of the model of Fig. 2.2.

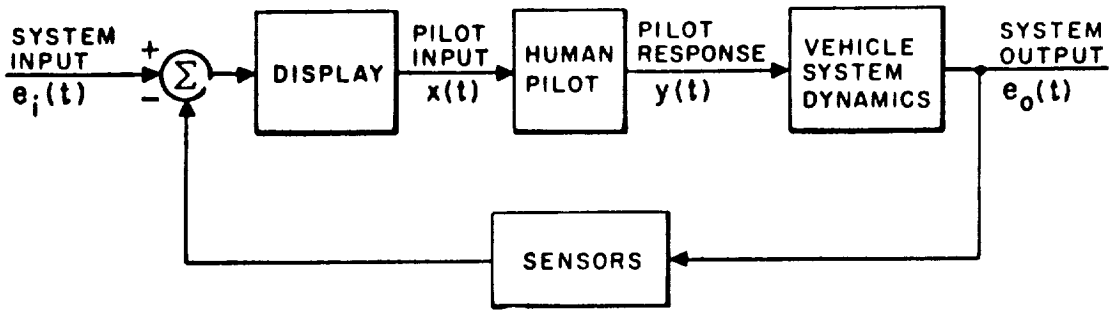

Figure 2.1.- Simplified block diagram of flight control system.

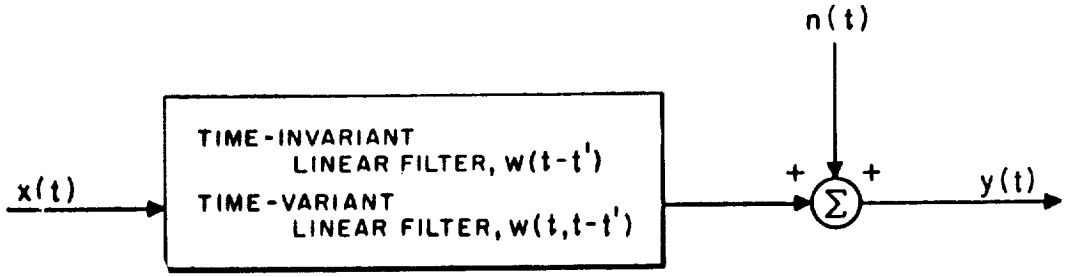

Figure 2.2.- Representations for human pilot - linear time-invariant or linear time-variant filter with output disturbed by noise, n(t).

The analysis techniques discussed in this report can be used to determine both time-invariant and time-variant weighting representations for human pilots in operational and simulated flight control situations. The techniques have obvious application to other problems of analysis of dynamic systems. We leave it to the reader to evaluate the applicability of the methods presented to other types of measurement problems.

III. DETERMINATION OF TIME-INVARIANT CHARACTERISTICS

A. WEIGHTING FUNCTION

First, consider the problem of determining a time-invariant weighting function for pilot characteristics. For the model of Fig. 2.2, the relation between pilot input and output can be written in terms of the convolution integral

$$y(t) = \int_{-\infty}^{t} w(t-t')\, x\,(t')\, dt' + n(t) \qquad (3.1)$$

where $x(t)$ is the input to the pilot; $y(t)$ is the output including the remnant noise $n(t)$; and $w(t-t')$ is the time-invariant weighting function that provides the least mean-square error approximation to pilot characteristics. The weighting function is to be determined from measurements made on $x(t)$ and $y(t)$.

The weighting function $w(t-t')$ is a representation of pilot characteristics in the time domain. We are not limited to a time domain representation, but could choose to represent pilot characteristics in some other domain, such as the frequency domain. In that case, the pilot's characteristics would be expressed in terms of a transfer function. In general, we can define a set of orthonormal functions $\phi_i(t)$ such that

$$\int_0^\infty \phi_i(t)\ \ \phi_j(t)\, dt = \begin{matrix} 1 \text{ for } i = j \\ 0 \text{ for } i \neq j \end{matrix} \qquad (3.2)$$

if these functions are complete we can approximate the pilot's weighting function with vanishingly small mean-square error by an infinite number of such functions. If this is done the system weighting function can be written

$$w(t) = \sum_{j=1}^{\infty} w_j\, \phi_j(t) \qquad (3.3)$$

and the system output becomes

$$y(t) = \sum_{j=1}^{\infty} \left[w_j \int_0^\infty \phi_j(t-t')\, x\,(t')\, dt' \right] + n(t) \qquad (3.4)$$

or

$$y(t) = \sum_{j=1}^{\infty} w_j z_j(t) + n(t) \qquad (3.5)$$

where $z_j(t)$ is the j^{th} integral in summation of Eq. (3.4). If the system weighting function is known, the coefficients w_j can be found by multiplying both sides of Eq. (3.3) by $\phi_j(t)$ and integrating over time. Because the $\phi_j(t)$ are orthogonal,

$$w_j = \int_0^{\infty} w(t)\ \phi_i(t)\ dt \qquad (3.6)$$

Equations (3.4) and (3.5) suggest a method for measurement in which a set of filters whose weighting functions are equal to the $\phi_j(t)$ of Eq. (3.3) are connected in parallel as shown in Fig. 3.1. The input to the pilot, $x(t)$ is fed to the filters. The filter outputs $z_j(t)$ are multiplied or weighted by the coefficients b_j and then summed to form $z(t)$. We call this parallel connection of filters a "mimic" and $z(t)$ the output of the mimic. For practical reasons, only a finite number of filters, say K, can be used in the mimic and the mimic output is

$$z(t) = \sum_{j=1}^{K} b_j z_j(t) \qquad (3.7)$$

The measurement problem now becomes one of finding the mimic coefficients that give the least mean-square difference (MSD) between mimic output and pilot output. It is also interesting to determine the relation between the mimic coefficients, b_j, and the coefficients of the series representation for the weighting function of Eq. (3.3), w_j. We assume for simplicity that the mean values of $x(t)$ and $n(t)$ are zero. Therefore, the mean values of $y(t)$ and of all the filter outputs will be zero. The coefficients b_j are determined so that the $\overline{\epsilon^2}$, the MSD between system output $y(t)$ and mimic output $z(t)$, is a minimum.

The MSD is determined by averaging the square of the difference between $y(t)$ and $z(t)$ over a period of T seconds' duration.

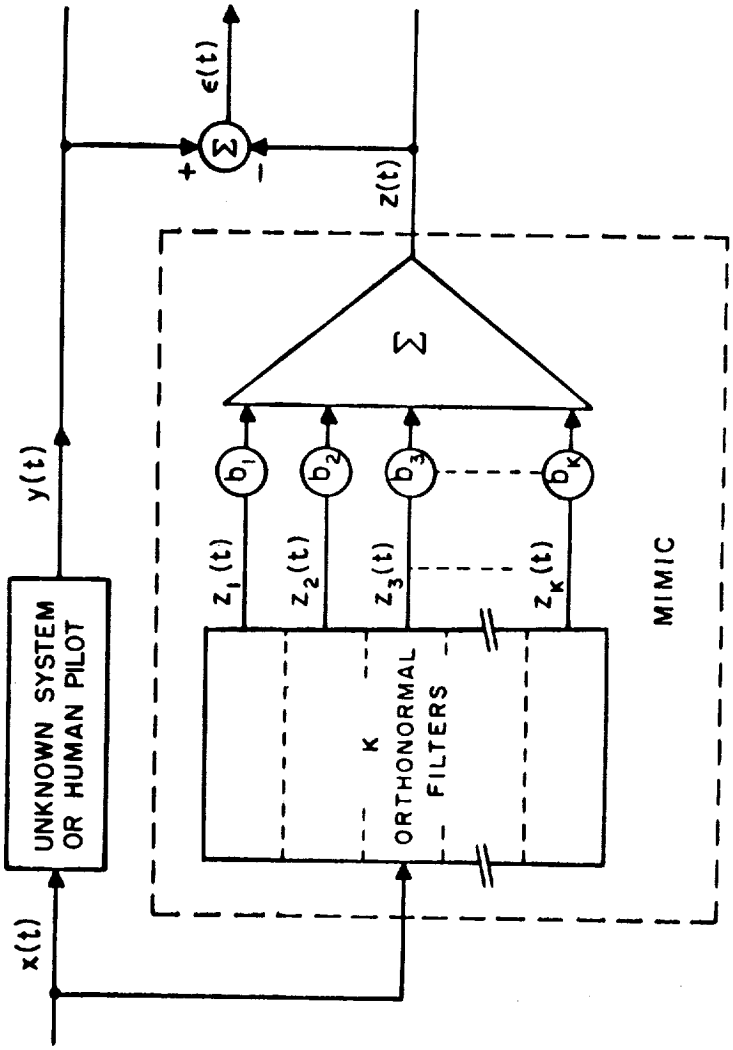

Figure 3.1.- Measurement by mimicking technique.

The difference or error is

$$\epsilon(t) = y(t) - z(t) = y(t) - \sum_{j=1}^{K} b_j z_j(t)$$

Its mean-square is (3.8)

$$\frac{1}{T}\int_0^T \epsilon(t)^2 dt = \overline{\epsilon^2} = \overline{[y(t) - \sum_{j=1}^{K} b_j z_j(t)]^2}$$

where the bar indicates that the average with respect to time is to be taken. The values of the coefficients b_j that minimize the MSD can be found by taking the derivative of $\overline{\epsilon^2}$ in Eq. (3.8) with respect to each b_j and setting the results equal to zero. Doing this, a set of K equations are obtained.

$$\begin{aligned}
\overline{z_1 z_1}\ b_1 + \overline{z_1 z_2}\ b_2 + \ldots \overline{z_1 z_K}\ b_K &= \overline{z_1 y} \\
\overline{z_2 z_1}\ b_1 + \overline{z_2 z_2}\ b_2 + \ldots \overline{z_2 z_K}\ b_K &= \overline{z_2 y} \\
\vdots \qquad\qquad \vdots \qquad\qquad \vdots \qquad\qquad \vdots & \\
\overline{z_K z_1}\ b_1 + \overline{z_K z_2}\ b_2 + \ldots \overline{z_K z_K}\ b_K &= \overline{z_K y}
\end{aligned} \tag{3.9}$$

where $\overline{z_i z_j}$ is the sample covariance of z_i and z_j for the period T and $\overline{z_i y}$ is the sample covariance of z_i and y for the same period.

Note that since it was assumed that the expected values of input x(t) and noise n(t) were zero, the expected value of z_i, z_j and y(t) will be zero. If the expected values of x(t) and n(t) were not zero, or were unknown, another equation would be required in the set of Eq. (3.9) and a constant would have to be added to the output of the mimic. The additional equation would be

$$a = m_y - \sum_{j=1}^{K} b_j m_j \tag{3.10}$$

where m_y is the sample mean of y(t) and m_j is the sample mean of $z_j(t)$. The covariances in Eq. (3.9) would have to be taken about these mean values and would be of the form

$$\overline{(z_i - m_i)(z_j - m_j)} \tag{3.11}$$

In the remainder of this report we assume that $x(t)$ and $n(t)$ have zero mean. The results obtained can be extended to the case in which the means are not zero by substituting expressions like the one in Eq. (3.11) for the covariances in Eq. (3.9).

In matrix notation Eq. (3.9) is written

$$\underline{L}\,\underline{b} = \underline{y} \tag{3.12}$$

where $\underline{L}$ is the K by K covariance matrix with the elements $\overline{z_i z_j}$; $\underline{b}$ is the $\underline{L}$ b column matrix of coefficients b_j; and $\underline{y}$ is the column matrix with elements $\overline{z_i y}$. If the mimic filters are chosen well, the weighting function of the mimic will be very nearly equal to that of the system, and

$$w(t) \sim \sum_{j=1}^{K} b_j \phi_j(t) \tag{3.13}$$

Since the mimic filters have known characteristics, the system weighting function can be determined, at least approximately, from Eq. (3.13) once the mimic coefficients have been computed. However, the b_j in Eq. (3.13) will not necessarily be equal to the w_j in Eq. (3.3). The b_j's are the coefficients of a finite series approximation to the pilot and are, in addition, subject to random variations resulting from the noise $n(t)$, whereas the w_j's are the coefficients of an infinite series approximation to the pilot's actual weighting function.

The values of the mimic coefficients that will be obtained in an actual measurement can be found by using Eq. (3.5) to expand $\underline{y}$ on the right side of Eq. (3.12). When this is done, the following matrix equation is obtained:

$$\underline{L}\ \underline{b} = \underline{L}\ \underline{w} + \underline{L}_{K+1}\ \underline{w}_{K+1} + \underline{n} \tag{3.14}$$

where $\underline{w}$ is the column matrix whose elements are the first K coefficients w_j of Eq. (3.3); $\underline{w}_{K+1}$ is the column matrix whose elements are the coefficients w_j for $j \geq K + 1$; $\underline{L}_{K+1}$ is the matrix of sample covariances $\overline{z_i z_j}$ for $i \leq K$ and $j \geq K + 1$; $\underline{n}$ is the column matrix whose elements are the sample

covariances of filter output $z_i(t)$ for $i \leq K$ and noise $n(t)$

The solution to Eq. (3.14) is:

$$\underline{b} = \underline{w} + \underline{L}^{-1}\ \underline{L}_{K+1}\ \underline{w}_{K+1} + \underline{L}^{-1}\ \underline{n} \tag{3.15}$$

or

$$\underline{b} = \underline{w} + \underline{g} + \underline{h} \tag{3.16}$$

where $\underline{g}$ and $\underline{h}$ are column matrices whose elements g_j and h_j are determined by the second and third terms on the right side of Eq. (3.15).

Thus, each mimic coefficient b_j is the sum of three components: the corresponding weight w_j of the expansion of system weighting function in terms of an infinite sum of orthonormal functions, Eq. (3.3); a bias g_j caused by approximating the system with a finite number of mimic filters; and a noise term h_j. Since the noise is uncorrelated with the input or with any of the mimic filter outputs, the expected value of $\underline{h}$ will be zero and

$$\underline{\beta} = \underline{w} + \underline{\gamma} \tag{3.17}$$

where $\underline{\beta}$ is a column matrix whose elements β_j are the expected values of the mimic coefficients and γ_j are the expected values of g_j.

For the special cases in which the input is white gaussian noise or an impulse, the expected covariance of one filter output with all other filter outputs will be zero (the filters have impulse responses that are orthogonal), and the expected value of $\underline{L}_{K+1}$ will be zero. In this case $\underline{\gamma}$ will be zero, β_j will equal w_j, and there will be no bias.

If the system can be represented exactly by a mimic composed of K filters, w_j for $j \geq K + 1$ will be zero, and therefore $\underline{\gamma}$ will be zero. The mimic coefficients will be unbiased and β_j will equal w_j. This will be true for all input signals.

B. DETERMINATION OF CORRELATION FUNCTIONS AND POWER SPECTRA

An autocorrelation or a cross-correlation function of two signals can be approximated by a linear combination of filter impulse response functions in much the same way as was the quasi-linear impulse response of the pilot (ref. 28). That is, the autocorrelation of the input signal $x(t)$,

$$R_{xx}(t') \sim \sum_{j=1}^{K} c_j \phi_j(t') \text{ for } t' > 0 \qquad (3.18)$$

where the $\phi_j(t')$ are the impulse responses of the mimic filters and the c_j are the weights applied to each $\phi_j(t')$.

If the $\phi_j(t')$ form a complete set of functions, the correlation function $R_{xx}(t')$ can be approximated with vanishingly small mean-square error if K in Eq. (3.18) is allowed to go to infinity. We will assume that the $\phi_j(t')$ are complete and orthonormal in the following discussion.

An expression for the c_j's can be obtained by multiplying both sides of Eq. (3.18) by $\phi_j(t')$ and integrating the product over all values of t' from zero to infinity. Because the functions are orthonormal, the only term of the summation that does not integrate to zero is the i^{th} term and

$$c_i = \int_0^\infty R_{xx}(t') \phi_i(t') \, dt' \qquad (3.19)$$

Equation (3.19) can be used to determine the weights of Eq. (3.18) if the autocorrelation function is known. Equation (3.18) can be used to compute the correlation function if the weights are known.

If the correlation function is not known, the weights can be computed directly from the signal $x(t)$ by using a method developed by Lampard (ref. 29). A set of mimic filters are excited by the signal $x(t)$, and the filter outputs are multiplied by $x(t)$. The average values of the resulting products are the desired weights. The output of the i^{th} filter is

$$z_1(t') = \int_0^\infty x(t-t') \phi_i(t') \, dt' \qquad (3.20)$$

By multiplying both sides by $x(t)$ and averaging, we obtain

$$\frac{1}{T}\int_0^T x(t)\, z_i(t)\, dt = \int_0^\infty \left[\frac{1}{T}\int_0^T x(t)\, x(t-t')\, dt\right] \phi_i(t')\, dt' \qquad (3.21)$$

The average value of $x(t)\, x(t-t')$, the second integral, is the autocorrelation function $R_{xx}(t')$ and

$$\overline{xz_i} = \frac{1}{T}\int_0^T x(t)\, z_i(t)\, dt = \int_0^\infty R_{xx}(t')\, \phi_i(t')\, dt' \qquad (3.22)$$

The integral on the right is identical with that in Eq. (3.19) and, thus,

$$c_i = \overline{xz_i} = \frac{1}{T}\int_0^T x(t)\, z_i(t)\, dt \qquad (3.23)$$

Once the weights c_j are determined, Eq. (3.18) can be used to compute the autocorrelation function $R_{xx}(t')$. Since the power density spectrum of $x(t)$, $S_{xx}(j\omega)$, is the Fourier transform of the autocorrelation function $R_{xx}(t')$ (ref. 14),

$$S_{xx}(j\omega) \sim \sum_{j=1}^{K} c_j\, \Phi_j(j\omega) \qquad (3.24)$$

where $\Phi_j(j\omega)$ is the Fourier transform of $\phi_j(t')$.

Cross-correlation functions of two signals can also be obtained using this method. One of the signals is used as the input to the mimic filter and the other is used as the multiplier of filter outputs.

C. DETERMINATION OF REMNANT

In general, the mimic will not account for all of the output of the system. The part not accounted for, the residual $\epsilon(t)$, is the difference between the system output $y(t)$ and the mimic output $z(t)$. The residual has two components: one results from the pilot's remnant $n(t)$ and the other from imperfect approximation of the pilot's weighting function, $w(t-t')$. If the pilot's weighting function is approximated with very little error, the residual will be almost entirely composed of the pilot's remnant.

If we carry out the squaring operation indicated in Eq. (3.8) and note that

$$\sum_{j=1}^{K} b_j \sum_{l=1}^{K} b_l \overline{z_j z_l} = \sum_{j=1}^{K} b_j \overline{z_j y} \qquad (3.25)$$

we obtain for the following expression for the mean-square or variance of the residual

$$s_\epsilon^2 = \overline{\epsilon^2} = s_y^2 - \sum_{j=1}^{K} \overline{z_j y} \qquad (3.26)$$

where s_y^2 is the variance of $y(t)$, i.e., $\overline{y(t)^2}$ Equation (3.26) can be used to determine the mean-square error of approximation to pilot characteristics, s_ϵ^2, once the mimic coefficients and covariances $\overline{z_j y}$ have been computed. If the mimic is a good approximation to pilot weighting function, most of the residual will result from pilot remnant $n(t)$.

The power spectrum of the residual can be computed in two ways. If the mimic transfer function is $M(j\omega)$ and the input and output power spectra, $S_{xx}(j\omega)$ and $S_{yy}(j\omega)$, have been determined, the residual spectrum can be determined from the relation

$$S_{\epsilon\epsilon}(j\omega) = S_{yy}(j\omega) - \left| M(j\omega) \right|^2 S_{xx}(j\omega) \qquad (3.27)$$

The second term on the right is the power spectrum of the output of the mimic. The difference between it and the power spectrum of the pilot's output is the power spectrum of the residual.

When Eq. (3.27) is used to determine the residual spectrum, errors in approximating S_{xx} and S_{yy} will result in errors in $S_{\epsilon\epsilon}$. A more accurate method for determining the residual spectrum is actually to obtain the residual signal $\epsilon(t)$ as shown in Fig. 3.1. Once the mimic coefficients have been determined, the input signal $x(t)$ can be fed to the mimic a second time, and the mimic output $z(t)$ obtained. By subtracting $z(t)$ from pilot output $y(t)$, the residual signal $\epsilon(t)$ is found. The power spectrum $S_{\epsilon\epsilon}(j\omega)$ is computed from $\epsilon(t)$ using the method discussed in the previous section. Since $\epsilon(t)$ consists largely of components of pilot's response that are not linearly correlated with pilot input, analysis of this signal may be useful for identification of nonlinearities in pilot characteristics.

IV. STATISTICAL PROPERTIES OF MIMIC COEFFICIENTS

A. DISTRIBUTION OF MIMIC COEFFICIENTS

The mimic coefficients are partial regression coefficients or pilot output $y(t)$ on each of the filter outputs $z_j(t)$. It is shown in standard statistical texts (refs. 21 and 22) that if the residual $\epsilon(t)$ is normally distributed, the mimic coefficients b_j will be normally distributed. The expected value of b_j is given by Eq. (3.17). The variance of b_j is

$$\text{Var}\,[b_j] = \frac{\sigma_\epsilon^2}{N s_{ju}^2} \tag{4.1}$$

where σ_ϵ^2 is the expected value of the variance of the residual error; N is the number of independent samples of the residual used in the computation of b_j. Note that N must be greater than K for Eq (4.1) to make sense, since at least K samples are needed to solve uniquely the K simultaneous equations required to determine the b_j. s_{ju}^2 is the sample variance of the part of the output of the j^{th} filter, that is uncorrelated with the other K-1 filter outputs and is equal to the j^{th} term on the diagonal of the inverse of the covariance matrix, $\underline{L}^{-1}$.

The variance of b_j depends upon the value of the variance s_{ju}^2 obtained in a particular measurement of b_j. The mean of b_j is independent of s_{ju}^2 and is equal to β_j. For each value of s_{ju}^2, b_j has a different normal distribution. Therefore, the probability density of b_j is conditional on s_{ju}^2 and is denoted $p[b_j|s_{ju}^2]$. $p[b_j|s_{ju}^2]$ is the conditional probability density of b_j given s_{ju}^2. Similarly, the variance of b_j is conditional on s_{ju}^2, and is denoted $\sigma_{bj|s}^2$. Using this notation, Eq. (4.1) may be written

$$\sigma_{bj|s}^2 = \frac{\sigma_\epsilon^2}{N\, s_{ju}^2} \tag{4.2}$$

The expected variance of b_j can be obtained by averaging $\sigma_{bj|s}$ in Eg. (4.2) over all values of s_{ju}^2. Thus, b_j is distributed with mean β_j

and variance σ_{bj}^2 given by

$$\sigma_{bj}^2 = \frac{\sigma_\epsilon^2}{N} \int_o^\infty \frac{1}{s_{ju}^2} p[s_{ju}^2]\, d[s_{ju}^2]$$

or

$$\sigma_{bj}^2 = \frac{\sigma_\epsilon^2}{N} E[1/s_{ju}^2] \tag{4.3}$$

where $E[1/s_{ju}^2]$ is the expected value of $1/s_{ju}^2$ and $p[s_{ju}^2]$ is the probability density of s_{ju}^2.

Denote the part of the output of the j^{th} filter that is uncorrelated with the other mimic filter outputs by $z_{ju}(t)$ and its variance by σ_{ju}^2 $z_{ju}(t)$ is the part of $z_j(t)$ that remains after the best linear combination of the other K-1 filter outputs is subtracted from $z_j(t)$. Assume that during the T-second long sample used to compute s_{ju}^2, there are M independent samples of $z_{ju}(t)$. If the system input is normally distributed with mean zero, the filter outputs will be normally distributed with mean zero and the quantity

$$\frac{Ms_{ju}^2}{\sigma_{ju}^2} \sim \chi^2 \tag{4.4}$$

will have approximately a χ^2 distribution with [M-(K+1)] degrees of freedom. K-1 degrees of freedom are lost in the computation of the part of $z_j(t)$ that is uncorrelated with the other filter outputs. Equation (4.3) can be rewritten in terms of χ^2 by using Eq. (4.4).

$$\sigma_{bj}^2 \sim \frac{\sigma_\epsilon^2 M}{N\, \sigma_{ju}^2} \int_o^\infty \frac{1}{\chi^2} p[\chi^2]\, d[\chi^2] \tag{4.5}$$

Carrying out the integration indicated in Eq. (4.5), we obtain

$$\sigma_{bj}^2 \sim \frac{\sigma_\epsilon^2 M}{N\, \sigma_{ju}^2 [M-(K+1)]} \quad \text{for } M \geq K+1 \tag{4.6}$$

Equation (4.6) is not a good approximation to $\sigma^2_{b_j}$ when M is nearly equal to or less than K+1. For M is this range the χ^2 assumption is not accurate.

Equation (4.1) gives the variance of the mimic coefficient when a particular value of s^2_{ju} is obtained in a measurement. The mimic coefficients will be normally distributed with this variance if the residual $\epsilon(t)$ is normal. The pilot's input and output need not be normal for the mimic coefficients to be normal. However, in Eq. (4.6) $\sigma^2_{b_j}$, the variance averaged over all values of s^2_{ju}, was derived under assumption that the input and output were normal. In the event the residual is not normal, the results obtained in this section will not be strictly correct. If the deviation from normality is not too great, these results should still provide good estimate of the statistical properties of the mimic coefficient.

B. CONFIDENCE LIMITS FOR MIMIC COEFFICIENTS

The results above can be used (1) to place confidence limits on β_j, the expected value of the mimic coefficients, once the sample mimic coefficients b_j have been obtained or (2) to test the significance of differences between two values of b_j. We consider two measurement situations: those in which σ_ϵ, the standard deviation of the residual error, is known and those in which σ_ϵ must be estimated. The usual assumptions of normality of system and mimic outputs are made.

If σ_ϵ is known, the variance of any measured value of b_j can be computed from Eq. (4.2). The conditional variance $\sigma^2_{b_j|s}$ is used rather than the expected variance $\sigma^2_{b_j}$ of Eq. (4.6), since in any measurement of b_j, s^2_{ju} is specified and can be determined from the covariance matrix $\underline{L}$. Eq. (4.2) requires knowledge of N, the number of degrees of freedom of the residual $\epsilon(t)$. The "sampling theorem" can be used to obtain a rough estimate of N (ref. 30). If $\epsilon(t)$ is limited to a bandwidth W_ϵ cycles per second, $2W_\epsilon$ independent samples per second are required to specify $\epsilon(t)$, and $2W_\epsilon T$ degrees of freedom are obtained in T seconds. If, as is usually the case, $\epsilon(t)$ is not limited to a bandwidth W_ϵ cycles per second, the

sampling theorem is not strictly applicable. Nonetheless, it is still useful for obtaining an estimate of N. To obtain such an estimate, the equivalent square bandwidth of $\epsilon(t)$ is used for W_ϵ in the expression for degrees of freedom. The equivalent square bandwidth of a low-pass signal is the bandwidth of a signal whose spectrum is rectangular with a magnitude equal to the peak of the spectrum of the original signal and with a bandwidth such that the energies of the two signals are the same. If the spectrum of $\epsilon(t)$ cuts off sharply, the equivalent square bandwidth approximation will be reasonably good. If it falls off gradually, the equivalent square bandwidth estimate will be in error, but still close enough to be useful. For example, for white noise filtered by a single low-pass RC filter, the estimate that $N = 2W_\epsilon T$ is low by a factor of approximately $\sqrt{2}$ (ref. 31). Estimates of M in Eq. (4.6) can be obtained using these same approximations.

Once $\sigma_{b_j|s}$ and b_j are computed, we can determine from tables of the normal distribution the probability that β_j lies within certain confidence limits. If two measurements of b_j are made from different samples of the signals $\sigma_{b_j|s}$ can be used to determine whether or not there is any significant difference between the coefficients. For example, if the expected values of the mimic coefficient β_j are the same for the two measurements, the probability is .95 that

$$b_{j2} - b_{j1} \leq 2 \sqrt{\sigma^2_{b_j|s1} + \sigma^2_{b_j|s2}} \qquad (4.7)$$

where b_{j1} and b_{j2} are the first and second measurements of a coefficient and the term on the right is the square root of the sum of the variances b_{j1} and b_{j2} (ref. 21).

In most measurement situations, σ_ϵ is not known and the sample standard deviation s_ϵ must be used. It can be computed from Eq. (3.26). It can be shown that the quantity

$$t = \sqrt{N - K}\,\frac{s_{ju}}{s_\epsilon}\,(b_j - \beta_j) \qquad (4.8)$$

has a Student's distribution with N-K degrees of freedom (ref. 21). Equation (4.8) involves only quantities that can be measured from samples

of the input and output signals and does not require knowledge of population characteristics. From tables of the Student's distribution, one can determine the probability that β_j lies outside prescribed confidence limits.

V. MEASUREMENT OF LINEAR TIME-VARYING SYSTEMS

A. REPRESENTATION OF TIME-VARYING SYSTEMS

The regression analysis technique can be used to determine the characteristics of time-varying systems provided the system to be measured does not change its characteristics too rapidly. The mimic coefficients are permitted to be functions of time to account for variation in system characteristics. Time-varying mimic coefficients are determined from Eq. (3.12), the same equation that is used to find the coefficients for time-invariant linear systems. However, to measure the variations in system characteristics, the coefficients must be determined from samples of the system and mimic filter output signals that are short compared to the length of time required for the system to change its characteristics. That is, during the T-second long sample used to compute the covariances of Eq. (3.12) the system must not have changed its characteristics significantly. If it has changed characteristics, the mimic will approximate the average characteristics of the system over the T-second long sample period.

The characteristics of a time-varying linear system, like that in Fig. 2.2, whose output is disturbed by noise can be represented by a time-varying weighting function. The output $y(t)$ of such a system is related to the input $x(t)$ by the convolution integral,

$$y(t) = \int_{-\infty}^{t} w(t,t-t')\, x(t')\, dt' + n(t) \qquad (5.1)$$

The function $w(t,t-t')$ is the system weighting function at time t and is the contribution that an impulse occurring at time t' would make to the output at time t (ref. 32).

We now show that a mimic whose coefficients are functions of time can approximate a time-varying system. Let the mimic be composed of filters whose impulse responses form a complete orthonormal set. At any time t the weighting function of a time-varying system, $w(t,t-t')$, can be approximated with vanishingly small mean-square error by an infinite number of

these filters. Thus, the system weighting function is

$$w(t,t-t') = \sum_{j=1}^{\infty} w_j(t)\, \phi_j(t-t')$$

and the system output is (5.2)

$$y(t) = \sum_{j=1}^{\infty} w_j(t)\, z_j(t) + n(t)$$

where $w_j(t)$ is the weight applied at time t to the j^{th} filter. In Eq. (5.2), the time-varying weighting function has been partitioned into a set of time-invariant filters and a set of time-variant coefficients $w_j(t)$ that weight the output of these filters.

Equations (5.2) are series expressions for the system weighting function and system output when an infinite number of orthonormal filters is used to approximate the system. When a finite number of filters is used in the mimic, the time-varying mimic coefficients $b_j(t)$ will not, in general, equal the $w_j(t)$ in Eq. (5.2).

If we assume that the system remains invariant during the time T required to measure the mimic coefficients, then the results obtained for time-invariant systems still apply. In particular, Eqs. (3.15) and (3.16) apply if we replace the time-invariant coefficients by time-varying coefficients,

$$\underline{b}(t) = \underline{w}(t) + \underline{L}^{-1}\, \underline{L}_{K+1}\, \underline{w}_{K+1}(t) + \underline{L}^{-1}\, \underline{n}$$

and (5.3)

$$\underline{b}(t) = \underline{w}(t) + \underline{g}(t) + \underline{h}$$

These equations relate the coefficients $b_j(t)$ of a finite mimic to the coefficients $w_j(t)$ of an infinite series approximation to the time-varying system.

B. SAMPLE LENGTH REQUIREMENTS

The crucial factor that determines the usefulness of the mimicking technique for measurement of time-varying systems is the length of the sample T that is required to obtain measurements of the mimic coefficients that have sufficiently small variance. If the coefficients can be determined with small variance from a short sample, the method will be highly useful. If a long sample is required, its usefulness is limited.

To determine how long a sample length T is required, we must first decide what confidence limits are desired, that is, we must specify the required value of σ_{bj}^2. Given a value of σ_{bj}^2 the sample length T required to achieve the desired σ_{bj}^2 can be determined. From Eq. (4.6) we see that the variance σ_{bj}^2 depends directly upon the ratio M/[M-(K+1)]. If M is much larger than K + 1, this ratio will be approximately unity and the variance can be approximated by the relation

$$\sigma_{bj}^2 \sim \frac{\sigma_\epsilon^2}{N\ \sigma_{ju}^2} \tag{5.4}$$

If we use the sampling theorem to relate N, the number of degrees of freedom, to T, the sample length, the following relation for T is obtained.

$$T \sim \frac{\sigma_\epsilon{}^2}{2W_\epsilon\ \sigma_{ju}^2\ \sigma_{bj}^2} \tag{5.5}$$

If M is not large compared to K + 1, Eq. (4.6) cannot be simplified, and the following expression for the variance must be used to determine T (using the sampling theorem).

$$\sigma_{bj}^2 \sim \frac{\sigma_\epsilon{}^2\ \ 2W_{ju}T}{2W_\epsilon T\ \sigma_{ju}^2\ [2W_{ju}T-(K+1)]} \tag{5.6}$$

where W_{ju} is the effective square bandwidth of $z_{ju}(t)$.

The quantities W_ϵ, W_{ju}, $\sigma_\epsilon{}^2$ and σ_{ju}^2 must either be known or estimated to determine T. In some cases, these quantities can be computed from

theoretical considerations alone. In other cases, preliminary measurements of system characteristics can be made from which these quantities can be estimated. Since the present objective is just to estimate the sample length T required to measure the b_j with given confidence limits and not to perform a statistical test of the significance of a particular measurement of the mimic, it is sufficient to use approximate values for the quantities upon which T depends.

VI. SELECTION OF MIMIC FILTERS

A. GENERAL CONSIDERATIONS

The mimic can be constructed of any of a large number of different types of filters including a set of narrow band-pass filters, a set of time delays (a tapped delay line) or a set of low-pass filters with real poles (simple exponential filters). The only constraint we shall impose on the choice of filters is that the filter impulse responses should be orthonormal. This restriction is imposed principally to simplify analysis of mimic capabilities and is not a necessary restriction.

The basic problem in measurement of time-varying systems is to obtain from short samples of data mimic coefficients that have small variance. The variance of the mimic coefficients depends upon the characteristics of the filters used in the mimic in a number of ways. By choosing the filters properly, the variance can be reduced, or, alternatively, the sample length required to achieve some specific variance can be shortened.

The mimic filters should be chosen so that the mimic accounts for almost all of that part of the system output that is linearly correlated with the input. By doing this, the residual variance σ_ϵ^2 will be reduced, thereby reducing $\sigma_{b_j}^2$. The filters also should be selected so that a few filters account for almost all of the system output. These new filters will have coefficients that will be large and the relative variability of the coefficients, σ_{b_j}/b_j, will be small. Finally, since $\sigma_{b_j}^2$ depends inversely upon σ_{ju}^2 and directly upon the ratio $M/[M-(K+1)]$, it is desirable to choose the filters so that their outputs are as nearly independent as possible (to make σ_{ju}^2 large) and so that M the number of degrees of freedom in the uncorrelated part of the filter output, is large compared to K + 1 (to make $M/[M-(K+1)]$ approach one). M can be made large by choosing filters of wide bandwidth whose outputs are uncorrelated. If a small number of filters is used, K will be small and it will be easier to achieve a ratio $M/[M-(K+1)]$ that approaches unity.

From the point of view of convenience and habit, perhaps the most natural choice of filters for the mimic is a set of narrow bandpass filters. The outputs of such a set of filters are approximately orthogonal for all inputs (provided T is large) and the mimic coefficients are the real and imaginary parts of the transfer function of the system being measured. But, a very large number of narrow band filters is required to represent typical systems with small residual variance and the number of degrees of freedom M of each filter output will, in general, be small. As a result, a large σ_{b_j} is to be expected when narrow band filters are used. One might think that because the outputs of narrow band filters are orthogonal, that the covariance matrix of Eqs. (3.9) and (3.12) would reduce to a diagonal matrix and solution for the mimic coefficients would be simple. This advantage is not obtained if short samples of signals are used to compute mimic coefficients. With short samples the off-diagonal terms of the sample covariance matrix will not, in general, be zero, and the full matrix equation must be solved.

B. A CLASS OF ORTHONORMAL FUNCTIONS

To achieve a good representation with a small number of filters, it is necessary to choose filters whose impulse responses resemble that of the system being measured. In most control situations, it appears that the linear part of human pilot characteristics can be approximated by transfer functions consisting of a delay, one to two lags, and frequently a lead, i.e.,

$$H(s) \sim \frac{K(s + s_{h\ell})\, e^{-\alpha s}}{(s + s_{h1})(s + s_{h2})} \qquad (6.1)$$

The poles and zeroes of approximations to pilot transfer functions are almost always found to be real or located very close to the real axis.

Thus, a reasonable choice of filters for use in a mimic would be a set of low-pass filters with real poles. These filters would have to be orthogonalized, but that is not difficult to accomplish.

Kautz (ref. 27) and Huggins (ref. 26) discuss a class of orthonormal filters that has a number of advantages and that we have found to be particularly useful. Sets of orthonormal filters belonging to this class are constructed from filters whose impulse responses are simple exponential functions, $e^{-s_1 t}$, and whose transfer functions are of the form $1/(s + s_1)$.

The Kautz procedure for orthogonalizing a set of exponentials is the following. If the first orthonormal function is a single exponential (it could be a sum of exponentials) with a pole at $s = -s_1$, it will have the transfer function

$$\Phi_1(s) = \frac{\sqrt{2s_1}}{s + s_1} \qquad (6.2)$$

If the second orthonormal function, $\Phi_2(s)$, is to contain a pole at $s = -s_2$, it can be shown that $\Phi_2(s)$ will be orthogonal to $\Phi_1(s)$ if it has the transfer function

$$\Phi_2(s) = \frac{\sqrt{2s_2}\ (s - s_1)}{(s + s_1)(s + s_2)} \qquad (6.3)$$

We can continue in this way, making each function have the poles of the previous function and zeroes that are the negatives of these poles, and obtain an orthonormal set composed of as many functions as we want. The general form for the i^{th} orthonormal function of this class is:

$$\Phi_i(s) = \frac{\sqrt{2s_i}\ (s - s_1)(s - s_2)\ldots(s - s_{i-1})}{(s + s_1)(s + s_2)\ldots(s + s_i)} \qquad (6.4)$$

C. POLE-ZERO LOCATIONS

We would expect, intuitively, that an orthonormal set of functions whose poles were located close to the poles of the system being measured would provide a good approximation to that system, with only a small number of filters being required. However, in advance of measurement, the

location of the poles and zeroes of the system being measured is known only approximately. The problem is to select the poles and zeroes of the orthonormal set of function so that the error in approximation remains small for the entire set of likely pole-zero configurations of the system or of the pilot.

Consider the problem of measuring a system whose transfer function is of the form

$$F(s) = \frac{\sqrt{2s_h}}{s + s_h} \qquad (6.5)$$

where the location of the pole s_h is not well known. Assume that the input is white noise of unit variance and that a set of orthonormal functions of the form of Eq. (6.4) is used to measure F(s).

It can be shown that for white noise inputs the expected mean-square error in approximating the system, the residual variance, is

$$\sigma_\epsilon^2 = \frac{(1 - s_h/s_1)^2(1 - s_h/s_2)2\ldots(1 - s_h/s_K)2}{(1 + s_h/s1)^2(1 + s_h/s_2)^2\ldots(1 + s_h/s_K)^2} \qquad (6.6)$$

where $-s_1, -s_2, \ldots -s_K$ are the locations of the poles of the orthonormal filters of the mimic (ref. 33). Each filter added to the mimic reduces the error variance by the factor

$$K_\epsilon = \frac{(1 - s_h/s_i)^2}{(1 + s_h/s_i)^2} \qquad (6.7)$$

In Fig. 6.1 K_ϵ is plotted versus s_h/s_i. If any of the poles of the mimic filters coincide with the pole of the system, σ_ϵ^2 goes to zero. To insure that a certain maximum error is not exceeded when s_h varies over a wide range (particularly since we actually do not know the location of s_h in advance of measurement), the poles of the mimic filters should be spaced

uniformly on a logarithmic scale.* That is, the poles should have the following values:

$$(-s_1, -ks_1, -k^2 s_1, \ldots, -k^{K-1} s_1)$$

With this choice of poles, if s_h is between s_1 and s_K, Eq. (6.6) will contain at least one term of the form of Eq. (6.7), that is, K_ϵ will be less than

$$K_{\epsilon max} = \frac{(1 - \sqrt{k})^2}{(1 + \sqrt{k})^2} \tag{6.8}$$

The residual variance σ_ϵ^2 from the two poles adjacent to s_h will be less than or equal to $K^2_{\epsilon max}$. Since K_ϵ is always less than one, the other filters will reduce the error further. Therefore, $K^2_{\epsilon max}$ is the maximum σ_ϵ^2 that will occur.

For example, if it were desired to achieve a residual error variance of less than one per cent of the variance of the system output, the poles of the mimic could be chosen as follows:

$$(-s_1, -4s_1, -16s_1, \ldots, -4^{(K-1)} s_1)$$

As long as s_h was located between s_1 and s_K (where $s_K = 4^{(K-1)} s_1$), the ratio s_h/s_i would never be greater than two nor less than one-half. If the s_h were located at the geometric mean of two analysis filter poles, the error would be maximum. From Fig. 6.1 we see that for the cases $s_h = 2s_i$ or $s_i/2$, if the two poles adjacent to s_h were the only poles of the mimic, the error would be $(0.11)^2$. The next two nearest poles would reduce the error by a factor of $(0.6)^2$ and the σ_ϵ^2 from the four filters would be less than 0.5 per cent.

---

* It should be noted that a set of filters whose poles are spaced uniformly on a logarithmic scale is not complete. However, for most practical problems, we are more interested in obtaining a good approximation with a small number of filters than in having the assurance that we can achieve very small error with a very large number of filters.

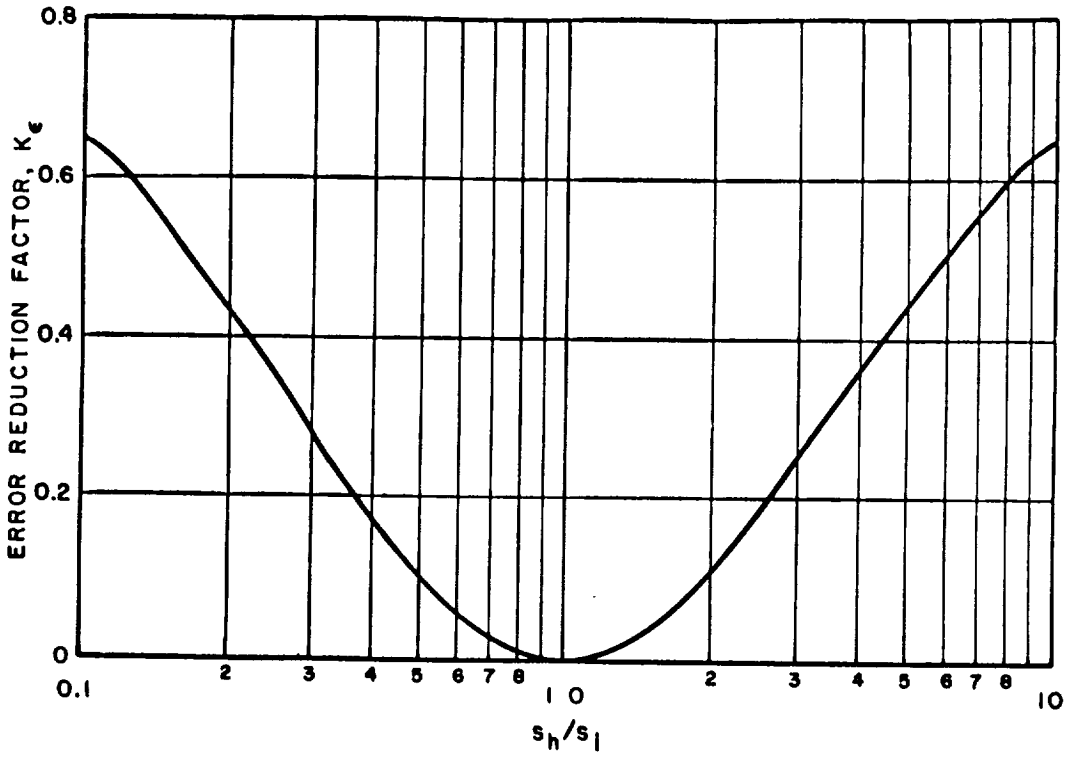

Figure 6.1.- Error reduction factor K_ϵ versus s_h/s_i.

If the system transfer function is of the form

$$F(s) = \frac{(s + s_{h_3})}{(s + s_{h_1})(s + s_{h_2})} \tag{6.9}$$

it can be expanded as a sum of two terms of the form of Eq. (6.5), each with a single pole. Figure 6.1 can be used to estimate the residual error variance in approximating each of these transfer functions separately. By making appropriate corrections for the scale factor associated with each component of the transfer function, an upper bound to the error in representing the composite transfer function can be obtained.

The upper bound is

$$\sigma_\epsilon \leq \sigma_{\epsilon_1} + \sigma_{\epsilon_2} \tag{6.10}$$

where σ_{ϵ_1} and σ_{ϵ_2} are the expected standard deviations of the errors in approximating the first and second components of F(s) of Eq. (6.9).

It is apparent from the preceding analysis that a large class of systems can be approximated accurately by mimics composed of a small number of filters (about 4 or 5), provided some care is exercised in locating the poles and zeroes of these filters. The locations of the poles and zeroes are not critical and they can be widely spaced. Wide spacing is an advantage, since it allows good approximations for a broad range of system pole locations. It is also apparent that to obtain as accurate an approximation to low-pass systems with a mimic composed of narrow band filters or time delays would require a much larger filter set than four or five.

The results presented above are useful in that they provide guides for selecting mimic filters. In the usual measurement situation, in which the locations of the poles and zeroes are not known, one cannot use the relations derived in this section to compute the error in approximation. Rather, Eq. (3.26), which involves only quantities derived from the actual

system or pilot input and output, should be used to compute the error. It should be noted, however, that it is not possible, even after a measurement has been made, to determine what part of the residual error is caused by imperfect approximation to the system's or pilot's transfer function and what part is caused by noise (or remnant) added to the output. One can only attempt to reduce the size of the part of the residual caused by imperfect approximation to a very small quantity by judicious choice of mimic filters. Fortunately, it does not appear to be too difficult to obtain filters that will provide rather accurate approximations to a wide variety of systems. A few trials with different filter sets should lead very rapidly to a satisfactory set.

D. COMPENSATION FOR TIME DELAY

When a small number of orthogonalized exponential filters are used in the mimic, systems that have a time delay term, $e^{-\alpha s}$, in their transfer functions may not be mimicked accurately. If the delay α is not very much smaller than the time constants of the system, significant errors in approximation will result. These errors can be reduced by using a larger number of filters in the mimic. A more efficient procedure is to compensate for the delay by adding a delay to the mimic so that the mimic filters do not have to reproduce the delay compenent.

One way of compensating for time delay is to delay the input to the mimic by τ seconds and the pilot's output by τ, $\tau - \delta$, $\tau - 2\delta$, $\tau - 3\delta$,..., $\tau - n\delta$ seconds. This procedure, in effect, gives several pilot outputs each advanced with respect to the input by a certain number of seconds, 0, δ, 2δ, 3δ,...,$n\delta$. Each of the advanced outputs can be used to compute the covariances $\overline{z_i y}$. In this way, several covariance vectors $\underline{y}$ Eq. (3.12), one for each value of delay compensation, are obtained. Eq. (3.12) can be solved for each $\underline{y}$ and a set of mimic coefficients can be obtained for each delay compensation. The delay compensation that yields the mimic coefficients that provide the least mean-square error approximation to the pilot's output can be taken to be the approximate delay of the pilot. This delay plus the corresponding mimic coefficients constitute the mimic parameters that best approximate pilot characteristics.

Delay compensation performed in the manner described does not result in a great increase in amount of computation. Only one covariance matrix $\underline{L}$ (Eq. (3.12)) has to be computed. Once its inverse is determined, it is relatively easy to solve for the several sets of mimic coefficients corresponding to the several $\underline{y}$.

VII. EXPERIMENTAL EVALUATION

Programs to perform all the mathematical operations required by the analysis technique were written for the PDP-1B digital computer (ref. 34). This is a medium size, high speed (5 microsecond memory access time), stored program machine. The programs were used to confirm the theoretical developments discussed in this paper. The programs are discussed in detail in the Appendix.

A. MEASUREMENTS OF VARIANCE OF MIMIC COEFFICIENTS

A single pole (digitally simulated) test filter of the form $1/(s+s_h)$ was analyzed using the computer programs. The pole of the test filter was located at $s = -1.0$ ($s_h = 1$). The filter was analyzed by a mimic composed of five filters of the form of Eq. (6.4). All five poles of the mimic filters were located at $s = -1.0$ ($s_i = 1$). Although a single filter of this kind would match the test filter exactly, a mimic composed of five filters was used to simulate more closely the situation likely to be encountered in an actual measurement problem.

The input signal $x(t)$ was digitally simulated white noise, a series of statistically independent pulses with approximately normal amplitude distribution. A pulse occurred every 0.1 second. Impulsive noise of the same type was added to the output of the filter. Except for this noise, the mimic could account for all of the output of the filter, and the variance of the residual error σ_e^2 was equal to the variance of the noise σ_n^2.

In Fig. 7.1 are shown values of σ_{b1} obtained from successive measurements of b_1 plotted against the normalized sample length, Ts_1, the sample length times the first mimic filter bandwidth. Between 50 and 150 samples of b_1 were used to determine σ_{b1}, the larger number of samples being used when the normalized sample length Ts_1 was small. Most of the values of σ_{b1} shown in Fig. 7.1 are for the case in which the ratio of the standard deviation of the residual to that of the uncorrelated filter output, σ_e/σ_{1u}, was equal to 0.41.

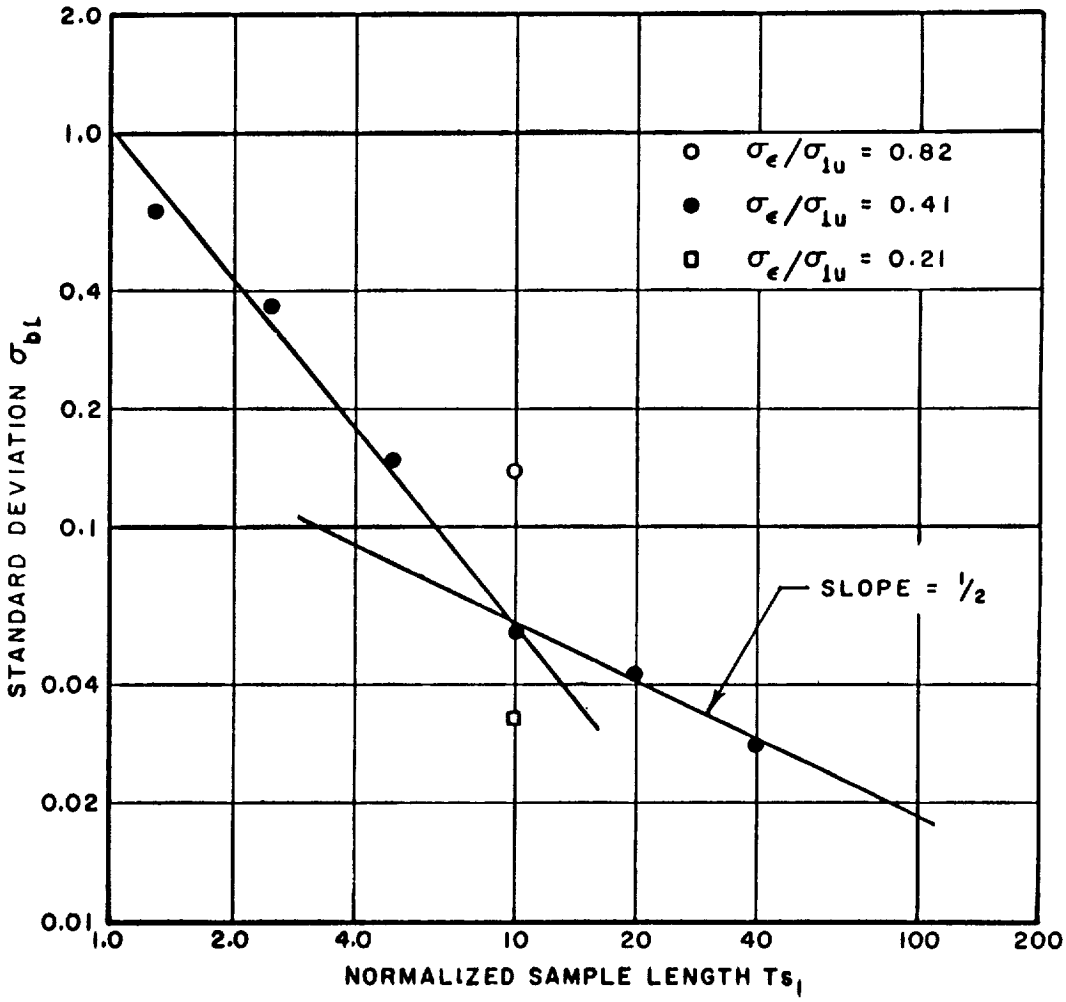

Figure 7.1.- Standard deviation of mimic coefficients versus normalized sample length Ts_l.

For values of Ts_1 greater than 10, σ_{b1} decreases inversely with $\sqrt{Ts_1}$. This is to be expected from Eq. (5.4) since for a single low-pass filter the equivalent square bandwidth of the mimic filter output, W_{1u}, is equal to $s_1/4$ and $2W_{ju}T$ in Eq. (5.4) is equal to $Ts_1/2$ For Ts_1 much greater than 10 this quantity will be greater than K+1, and from Eq. (5.6).

$$\sigma_{b1} \sim \frac{\sigma_\epsilon}{\sqrt{N}\,\sigma_{1u}} \sim \frac{\sigma_\epsilon}{\sqrt{2W_\epsilon T}\,\sigma_{1u}} \qquad (7.1)$$

For Ts_1 less than ten, σ_{b1} increases more rapidly than $1/\sqrt{Ts_1}$. Apparently $2W_{1u}T$ (or $Ts_1/2$) is sufficiently small so that the denominator term $[2W_{ju}T-(K+1)]$ dominates the behavior of Eq. (5.6). However, σ_{b1} does not tend to infinity as T decreases to very small values as would be predicted from Eq. (5.6). The reason probably lies in the inaccuracy of the assumptions that the filter outputs have a χ^2 distribution and that the sampling theorem gives the number of degrees of freedom.

Also shown for Ts_1 equal to ten are values of σ_{b1} obtained when the ratio $\sigma_\epsilon/\sigma_{1u}$ is increased and decreased by a factor of two from the value in Eq. (7.1). Values for σ_{b1} approximately twice as large and half as large as the central value of σ_{b1} were obtained. This agrees with Eq. (5.6).

B. MEASUREMENT OF TIME-INVARIANT FILTERS

A number of digitally simulated test filters were analyzed with a set of five mimic filters of the form of Eq. (6.4) whose poles were located at s = -.055, -.167, -0.5, -1.5, -4.5. The impulse responses of these filters are in Fig. 7.2. This set of mimic filters was chosen because its poles are logarithmically spaced, they span a wide range, and yet are not too far apart. The discussion in Section VI indicates that such a set of mimic filters should be capable of measuring a wide range of systems with relatively small error.

Several input signals were used including an impulse, impulsive noise, and impulsive noise filtered by 1/(s + 5.0). The filtered noise input is

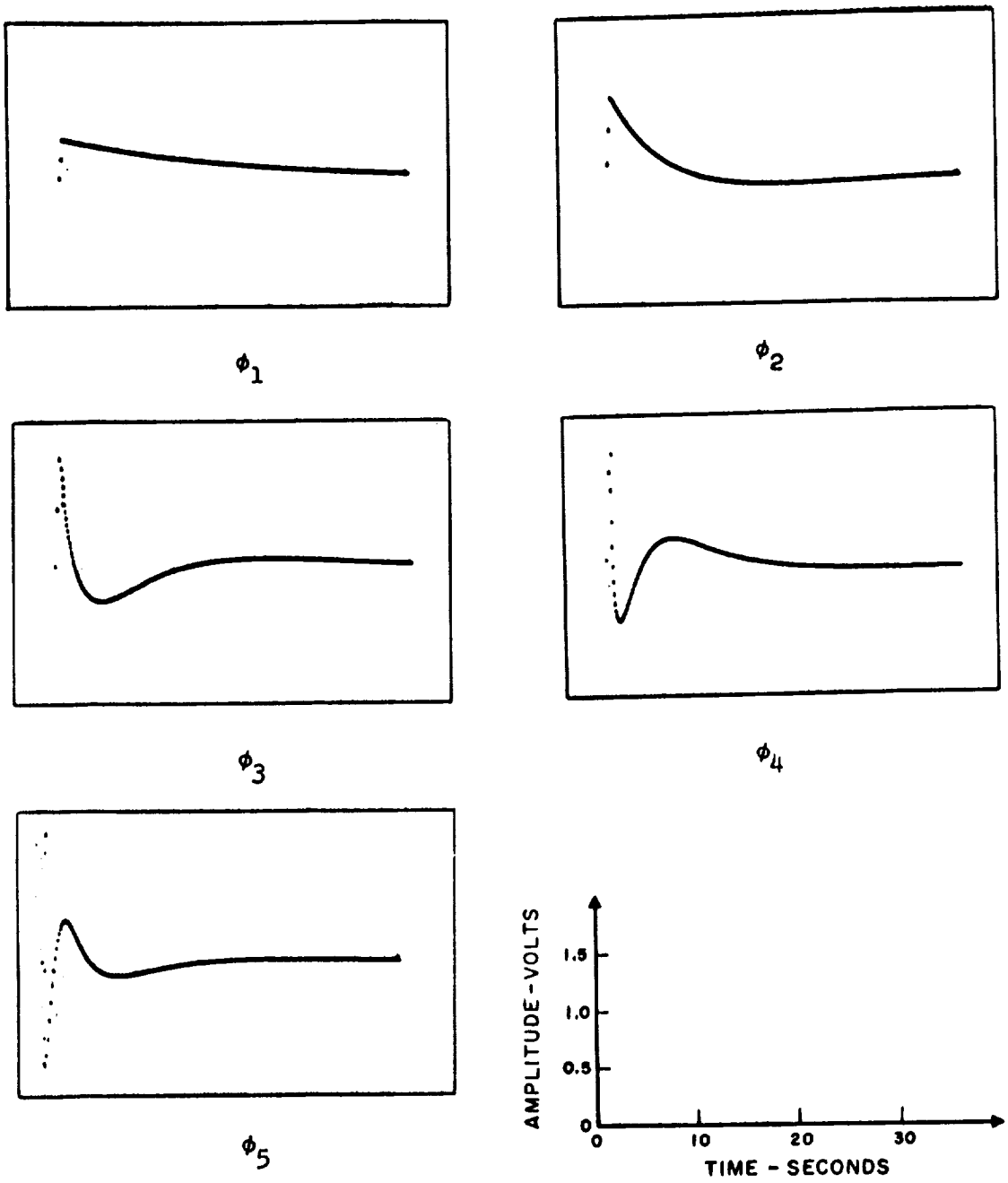

Figure 7.2.- Impulse responses of the mimic filters used in evaluation of measurement technique. Poles are at s = -0.055, -0.167, -0.5, -1.5, -4.5. The sampling interval was 0.1 second. The impulse was applied at t = 0.1 second.

similar to the pilot input in many control situations. The measurements were made both with and without impulsive noise added to the test filter output (to simulate pilot remnant). A sample length T of 48 seconds was used in all measurements. The integral-square error (ISE) in the impulse response relative to the integral-square of the impulse response was computed. Where applicable, the relative ISE in the response to an impulse filtered by $1/(s + 5.0)$ was also computed. It should be noted that when an impulse is used as the input for measurement purposes, the mimic coefficients obtained should be the expected values of the mimic coefficients, β_j, and the measured ISE should be the expected value of the residual variance, σ_ϵ^2.

The poles and zeroes of the digital test filters were located as shown in Fig. 7.3. Also shown in the figure are the locations of the poles of the mimic filters. Four of the test filter poles were located midway on a logarithmic scale between the two adjacent mimic filter poles. For one-pole test filters, at least, the error should be greater when the test filter pole is midway between the adjacent analysis filter poles than when it is closer to one of the poles than to the other. The test filter pole at $s = -0.5$ coincides with one of the mimic filter poles and, therefore, the one-pole test filter with this pole should be mimicked with no error. Two of the one-pole test filter poles were located outside the range spanned by the mimic poles. We would expect the error to be greatest for these two test filters. The transfer functions of the two-pole and the two-pole and one-zero test filters are similar to those of human pilots in many control situations.

1. Measurement Digital Filters with Impulse Inputs.

   a. Measurement Conditions.

      (1) Test Filters: variety of digital filters, one pole, two pole, two pole plus zero as shown in Fig. 7 3.

      (2) Mimic Filter Poles: $s = -.055, -.167, -.5, -1.5, -4.5$.

      (3) Input for measurement of coefficients: an impulse.

      (4) Input for measurement of error: an impulse.

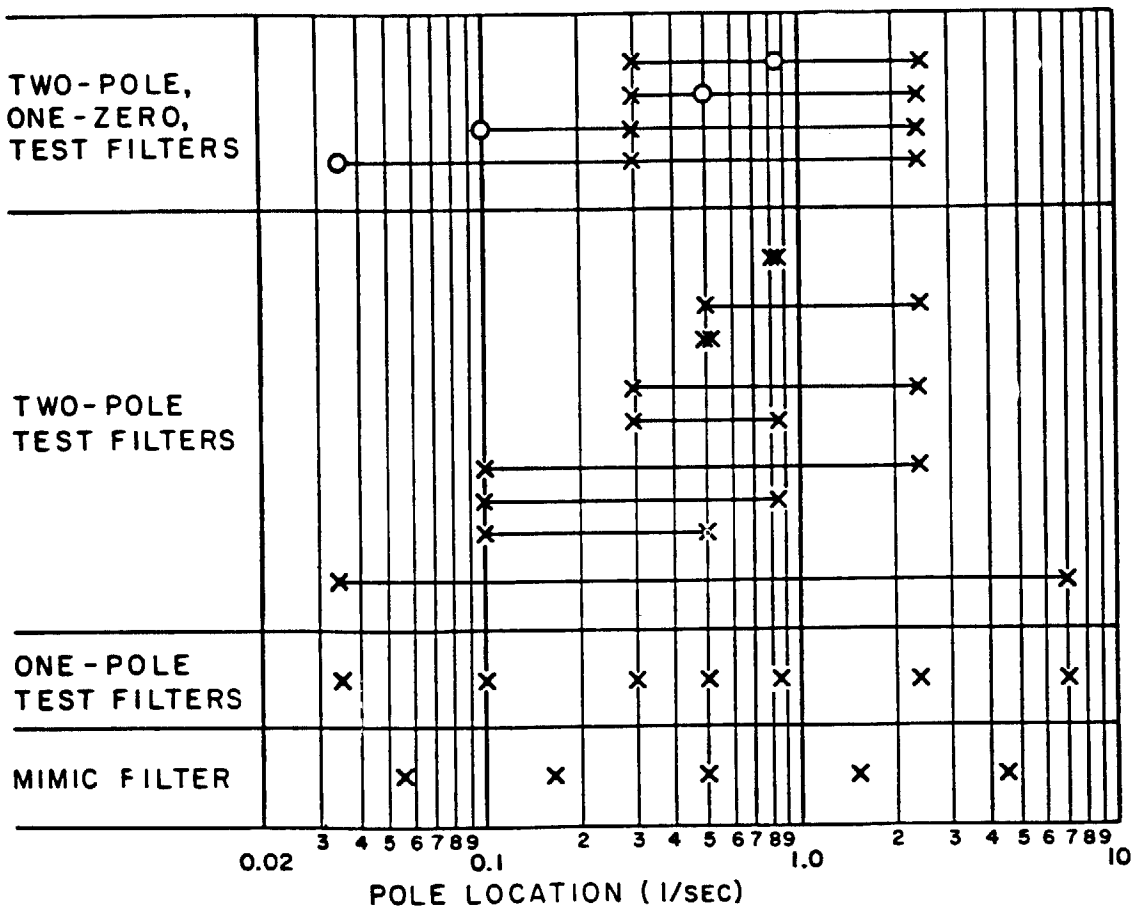

Figure 7.3.- Pole-zero locations of digital test filters and mimic filters.

(5) Sample length: 48 seconds.

(6) Sampling interval: 0.1 second.

b. Results.

In Table 7.1 are the mimic coefficients and the relative ISE in approximating the impulse responses of the one-pole test filters. The errors are less than one percent except for the filter whose pole is at s = -7.0, which is outside the range spanned by the mimic poles. The large error in approximating this filter is caused, in part, by digital approximation errors. The digital sampling interval is only slightly less than the time constant of the filter. The error for the test filter with pole at s = -.5 is very small. The difference between the measured error and the expected error of zero is probably due to round off and truncation errors incurred in the course of computation. Note that as the pole of the test filter increases the higher order mimic coefficients increase and the low order mimic coefficients decrease.

In Table 7.2 are the relative ISE for the two-pole test filters, and the two poles, one zero test filters. For both of these types of filters the error is almost always less than one percent and is never greater than one and one-half percent. Thus, with the exception of the one-pole filter with s = -7.0, all of the filters tested can be measured with less than one and one-half percent error with a single set of mimic filters. This result is obtained for filters whose poles and zeroes span a 200 to 1 range

2. Measurement of Digital Filters Having Time Delay with Impulse and Random Inputs.

a. Measurement Conditions.

(1) Test Filters:

1) $e^{-0.1s}/(s+0.3)$
2) $e^{-0.1s}/(s+2.5)$
3) $e^{-0.1s}/(s+0.3)(s+2.5)$
4) $e^{-0.1s}(s+.833)/(s+0.3)(s+2.5)$

TABLE 7.1 - ANALYSIS OF ONE-POLE DIGITAL FILTERS WITH IMPULSE INPUTS.
MIMIC FILTER POLES AT s = -.055, -.167, -.5, -1.5, -4.5.
MIMIC COEFFICIENTS AND RELATIVE INTEGRAL SQUARE IMPULSE RESPONSE ERROR.

TEST FILTER POLE	b_1	b_2	b_3	b_4	b_5	RELATIVE INTEGRAL-SQUARE ERROR
$\sqrt{.07}/(s + .035)$	.9775	-.1663	.0678	-.0317	.0222	0.736 %
$\sqrt{.2}/(s + 0.1)$	.9557	.2823	-.0536	.0212	-.0137	0.139 %
$\sqrt{.6}/(s + 0.3)$	.7228	.6683	.1900	-.0334	.0196	0.081 %
$\sqrt{1}/(s + 0.5)$	.5962	.6992	.4029	.0019	.0029	0.002 %
$\sqrt{1.666}/(s + 0.833)$	.4818	.6567	.5695	.1406	-.0288	0.091 %
$\sqrt{5.0}/(s + 2.5)$	.2916	.4694	.6362	.5696	.1710	0.26 %
$\sqrt{14.0}/(s + 7.0)$	.1792	.3034	.4839	.6780	.5781	5.12 %

TABLE 7.2 - ANALYSIS OF TWO-POLE DIGITAL FILTERS.

MIMIC FILTER POLES SAME AS IN TABLE 7.1.

FILTER	RELATIVE INTEGRAL-SQUARE ERROR IMPULSE RESPONSE
$\frac{1}{(s + .035)(s + 7.0)}$	1.37%
$\frac{1}{(s + 0.1)(s + 0.5)}$	0.26 %
$\frac{1}{(s + 0.1)(s + .833)}$	0.15 %
$\frac{1}{(s + 0.1)(s + 2.5)}$	0.22 %
$\frac{1}{(s + 0.3)(s + .833)}$	0.62 %
$\frac{1}{(s + 0.3)(s + 2.5)}$	0.73 %
$\frac{1}{(s + 0.5)(s + 0.5)}$	1.21 %
$\frac{1}{(s + 0.5)(s + 2.5)}$	0.05 %
$\frac{1}{(s + .833)(s + .833)}$	0.05 %
$\frac{(s + .035)}{(s + 0.3)(s + 2.5)}$	0.16 %
$\frac{(s + 0.1)}{(s + 0.3)(s + 2.5)}$	0.16 %
$\frac{(s + 0.5)}{(s + 0.3)(s + 2.5)}$	0.14 %
$\frac{(s + 0.833)}{(s + 0.3)(s + 2.5)}$	0.11 %

(2) Mimic Filter Poles: same as before.

(3) Inputs for measurement of coefficients:

1) Impulse
2) Unfiltered Impulsive Noise
3) Filtered Impulsive Noise
4) Unfiltered Noise Input with Unfiltered Noise added to Test Filter Outputs to Simulate Pilot Remnant
5) Filtered Noise Input with Unfiltered Noise for Remnant. The input was filtered by $1/(s + 5.0)$.

(4) Inputs for measurement of error: an impulse and an impulse filtered by $1/(s + 5.0)$.

(5) Sample length: 48 seconds.

(6) Sampling interval: 0.1 second for inputs (1), (2), and (3); 0.05 second for inputs (4) and (5).

b. Comparison of Results Obtained with Different Inputs.

Mimic coefficients were computed for each of the four test filters when excited by each of the input signals listed above. For each set of mimic coefficients the relative ISE in approximating the response of the test filters to an impulse or to a filtered impulse was computed. These errors are in Table 7.3. The ratio of remnant noise power to test filter output power (before addition of noise) is indicated in the table for those measurements in which remnant noise was added. All errors shown in Table 7.3 are for the case in which the 0.1 second delay of the test filter is compensated for exactly by the mimic.

As would be expected, the errors obtained with impulse inputs (Table 7.3, Column I) and unfiltered noise inputs without remnant (Column II) are nearly equal. The mimic coefficients for these two inputs were also nearly equal. This close match in results is expected since the unfiltered noise

TABLE 7.3 - ANALYSIS OF FOUR TYPICAL FILTERS

COMPARISON OF RELATIVE INTEGRAL-SQUARE ERRORS FOR MEASUREMENTS WITH IMPULSE, UNFILTERED NOISE AND FILTERED NOISE INPUTS WITH AND WITHOUT NOISE ADDED TO FILTER OUTPUT

TEST FILTER	I	II	III	IV	V	VI
	IMPULSE INPUT	UNFILTERED NOISE INPUT	FILTERED NOISE INPUT	UNFILTERED NOISE INPUT	FILTERED NOISE INPUT	
	IMPULSE RESPONSE ERROR	IMPULSE RESPONSE ERROR	FILTERED IMPULSE RESPONSE ERROR	IMPULSE RESPONSE ERROR	IMPULSE RESPONSE ERROR	FILTERED IMPULSE RESPONSE ERROR
(1) $\frac{1}{(s+0.3)}$	.08 %	.09 %	.10 %	.13 % (14% rem.)	.33 % (27% remnant)	.30 %
(2) $\frac{1}{(s+2.5)}$	.26 %	.22 %	.09 %	.17 % (9% rem.)	.46 % (25% remnant)	.26 %
(3) $\frac{1}{(s+0.3)(s+2.5)}$	.07 %	.10 %	.14 %	.80 % (22% rem.)	.10 % (35% remnant)	.10 %
(4) $\frac{(s+0.833)}{(s+0.3)(s+2.5)}$	.11 %	.12 %	.27 %	.22 % (10% rem.)	1.5 % (40% remnant)	1.8 %

input is composed of a series of statistically independent impulses having approximately normal amplitude distribution.

The small differences between the impulse and the unfiltered noise measurements results are probably caused by end effects. In the impulse measurements the response of test filter and mimic filters died out to zero during the 48 second period used to compute the mimic coefficients. In the noise measurements input excitation was applied for the entire 48 second period and the transients did not die out.

In Column III of Table 7.3 are the errors in the filtered impulse response obtained when the mimic coefficients were measured with a filtered noise input (without remnant). The errors with all four test filters are considerably less than one percent and not of great significance. The errors are, however, somewhat different from the impulse response errors of Column II which were obtained by using unfiltered noise to measure the mimic coefficients. The greatest change in error occurred with the two filters that had greatest bandwidth, Filters (2) and (4). This result is expected since the response of these two filters to an impulse filtered by $1/(s + 5.0)$ was considerably different from the response to an unfiltered impulse. The high frequency content was reduced greatly and the energy in the filtered impulse response was considerably less than the energy in the impulse response.

The integral-square errors in impulse response obtained when the mimic coefficients are measured with unfiltered noise input and with remnant noise added to the filter output are in Column IV of Table 7.3. The errors are all less than one percent. With one exception they are greater than the errors in Column I obtained with coefficients measured with impulse input. This result is to be expected since the errors with impulse inputs are the minimum that can be achieved.

For Filter (2) a smaller error was obtained with unfiltered noise input plus remnant than with impulse input. This filter had a bandwidth of 2.5 radians per second. The impulse measurements were made with a digital sampling interval of 0.1 second; the noise measurements with a sampling interval

of 0.05 second. The decrease in sampling interval is probably responsible for the somewhat smaller error. When the sampling interval is .05 second, the digital test filter approximates much more closely the filter $1/(s + 2.5)$ than when the sampling interval is 0.1 second. For the other test filters, which have narrower bandwidth, the change in sampling interval does not result in as important a change in the test filter.

The results with filtered random inputs plus remnant in Columns V and VI are of considerable interest because this test situation corresponds most closely to that usually encountered in measurement of pilot dynamics. For all four filters, the impulse response errors in Column V are greater than the impulse response errors in Column IV obtained with unfiltered noise. There are two reasons for this increase: (1) The remnant with filtered noise was considerably greater than that with unfiltered noise; and (2) the use of filtered noise input results in attenuation of the high frequency portion of the test filter output used to measure the mimic coefficients. However, the high frequency portion of the impulse response is not attenuated. It is probably the high frequency portion of the test filter impulse response that is not being mimicked as accurately and which contributes to the increase in error. Except for Filter (4), the errors are considerably less than one percent. For Filter (4), the error is about two percent. However, note that the remnant was 40 percent for this measurement.

In Table 7.4 are the mimic coefficients for Filter (4) obtained with each of the input signals. The first four coefficients are of importance. The fifth coefficient is small. The coefficients obtained with the first three input signals are all very nearly the same. The deviations from the coefficients obtained with impulse inputs are in the third decimal place. When remnant is added, the deviations became larger. For the filtered random input plus remnant rather large differences in coefficients are observed. However, the remnant power was 40 percent of the test filter output power.

c. Effects of Time Delay.

The four filters used in this experiment had a time delay of 0.1 second. This delay must be compensated in the measurement of filter characteristics.

TABLE 7.4 - MIMIC COEFFICIENTS FOR FILTER (4) $(s + 0.833)/(s + 0.3)(s + 2.5)$

OBTAINED WITH SEVERAL INPUT SIGNALS

INPUT	REMNANT	b_1	b_2	b_3	b_4	b_5	RELATIVE INTEGRAL-SQUARE IMPULSE RESPONSE ERROR
IMPULSE	--	.3204	.3641	.2716	.1770	.0558	.11 %
UNFILTERED NOISE	--	.3212	.3670	.2715	.1790	.0522	.12 %
FILTERED NOISE	--	.3171	.3659	.2700	.1805	.0608	.14 %
UNFILTERED NOISE	10 %	.3146	.3760	.2600	.1771	.0467	.22 %
FILTERED NOISE	40 %	.2844	.4136	.2437	.1415	.0460	1.5 %

The results given in Table 7.3 are for the case in which the delay is compensated exactly. In Table 7.5 are relative integral-square errors for different amounts of delay compensation.

The experimental conditions in Table 7.5 include unfiltered and filtered random inputs with remnant added. The error has been computed with impulse inputs and with filtered impulse inputs. The delay compensation is in increments of 0.05 second. If a digital sampling interval of 0.1 second were used, one may not be able to reduce the error in delay compensation to less than 0.05 second. In Table 7.5 deviation in delay compensation from the perfect compensation of 0.1 second is shown. This deviation is equal to the delay in the mimic minus the delay in the test filter.

If the delay deviation is negative, the mimic has a shorter delay than the test filter and the mimic responds before the test filter. Initially, the mimic attempts to suppress its response because there is no output from the filter. However, when the test filter begins to respond, the mimic must attempt to match it. If the delay deviation is positive, the mimic has more delay than the test filter and the mimic responds after the test filter. The mimic cannot match the initial part of the test filter response because it has not yet received its input. This initial part of the test filter response cannot be cancelled by the mimic and represents an irreducible error.

In Fig. 7.4 photographs of the response of Filter (4) to an impulse input are shown. Also shown in the figure are the errors in response that result with different amounts of delay compensation. The mimic coefficients used to obtain these response errors were those computed with filtered random inputs plus remnant and are the coefficients that gave the relative error scores shown for Filter (4) in Table 7.5.

As can be seen from Fig. 7.4, the filtered impulse response of the test filter rises smoothly from zero and the initial values of the response are of relatively small magnitude. Hence, the integral-square errors are not highly sensitive to the amount of delay compensation. In fact, in some cases, smaller errors are observed with delay compensation somewhat different from perfect

TABLE 7.5 - EFFECTS OF TIME DELAY ON INTEGRAL-SQUARE ERROR

TEST FILTER	$\Delta\alpha$ DELAY DEVIATION (MIMIC DELAY - TEST FILTER DELAY) SECONDS	UNFILTERED NOISE INPUT		FILTERED NOISE INPUT		
		REMNANT	IMPULSE RESPONSE ERROR	IMPULSE RESPONSE ERROR	REMNANT	FILTERED IMPULSE RESPONSE ERROR
(1) $\frac{e^{-0.1s}}{(s+0.3)}$	+0.10	14 %	5.3 %	6.6 %	27 %	0.92 %
	+0.05		1.6 %	1.4 %		0.22 %
	0		0.13%	0.33%		0.30 %
	-0.05		1.0 %	1.1 %		0.23 %
(2) $\frac{e^{-0.1s}}{(s+2.5)}$	+0.05	9 %	12 %	12 %	25 %	1.8 %
	0		0.17%	0.46%		0.26 %
	-0.05		10 %	11 %		1.9 %
(3) $\frac{e^{-0.1s}}{(s+0.3)(s+2.5)}$	+0.05	22 %	1.2 %	0.31%	35 %	0.28 %
	0		0.80%	0.10%		0.10 %
	-0.05		1.1 %	0.32%		0.28 %
(4) $\frac{e^{-0.1s}(s+.833)}{(s+0.3)(s+2.5)}$	+0.10	10 %		25 %	40 %	4.8 %
	+0.05		5.8 %	6.4 %		1.8 %
	0		0.22%	1.5 %		1.8 %
	-0.05		5.7 %	7.1 %		2.8 %
	-0.10			13 %		5.8 %

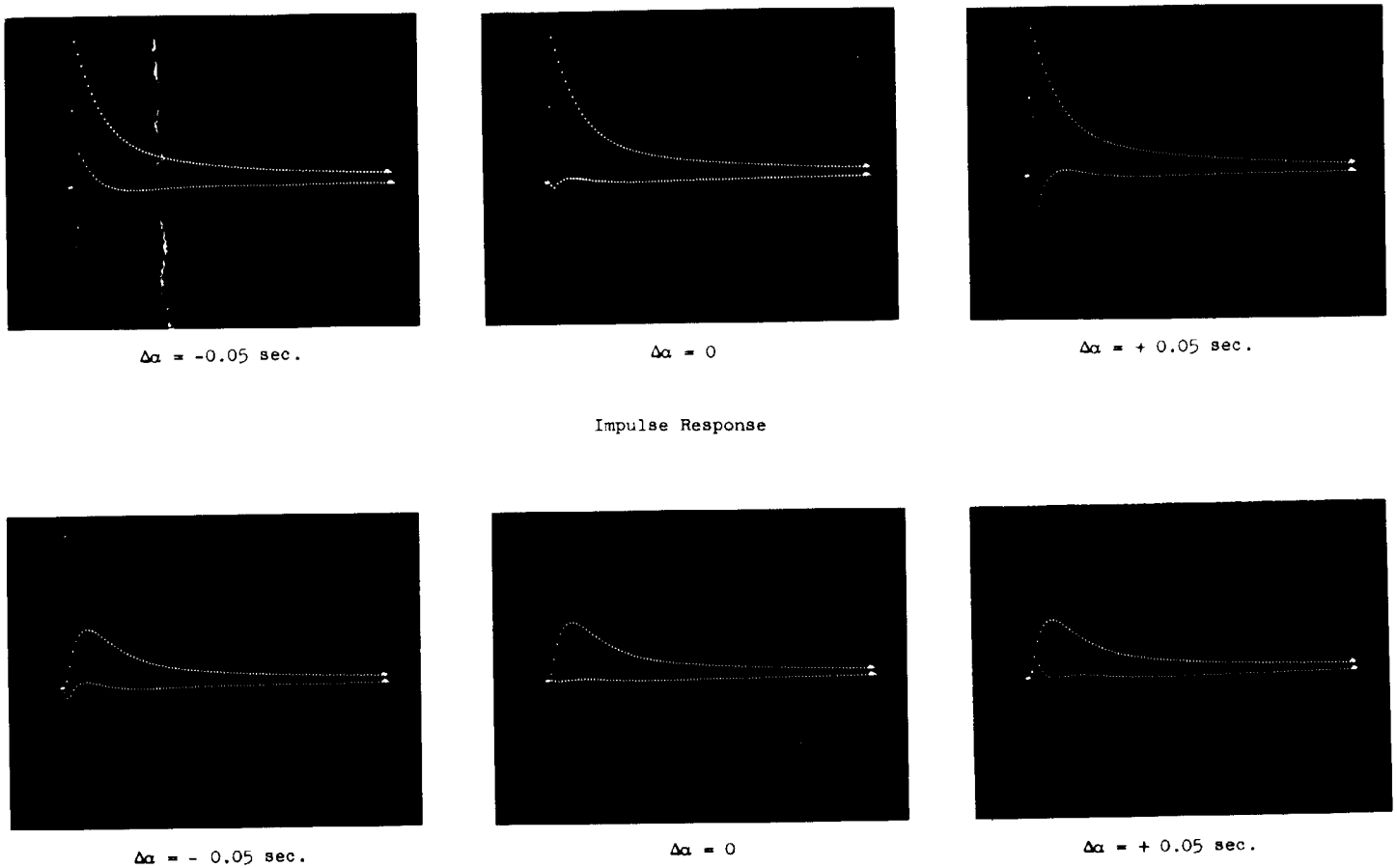

Figure 7.4.- Response (upper curve in each photograph) of filter (4) to an impulse and filtered impulse and error (lower curve) in response for three values of delay deviation. Mimic coefficients were determined with filtered noise input and 40 percent remnant. Ten seconds of response shown.

delay compensation. The impulse response of the test filter rises abruptly and the initial values of the responses are large. Hence, the integral-square error is highly sensitive to delay compensation. Least error is obtained with perfect delay compensation.

We see from Table 7.5 that when unfiltered noise is used as the input, the smallest error is always obtained with perfect delay compensation. If the test filter has a single pole or if the number of poles exceeds the number of zeroes by one, the impulse response of the test filter will have an initial discontinuity. We can approximate the filter impulse response by a simple decaying exponential. Call the time constant of the exponential the "effective time constant" of the filter. The relative ISE is, to a first approximation, equal to the magnitude of the ratio $|\Delta\alpha|/\tau_{eff}$, where $\Delta\alpha$ is the delay deviation and τ_{eff} is the effective time constant of the filter.

Test Filters (2) and (4) have small effective time constants. The ratio $|\Delta\alpha|/\tau_{eff}$ is large for $\Delta\alpha$ equal to $\pm$ .05 second and the relative errors are large. Test filter (1) has a large effective time constant and $|\Delta\alpha|/\tau_{eff}$ is small for $\Delta\alpha$ equal to $\pm$ .05 second. The relative errors in impulse response are small.

If the number of test filter poles exceeds the number of zeroes by more than one, the impulse response will begin at zero and rise smoothly. The ISE will not increase greatly with the delay deviation $\Delta\alpha$ provided $\Delta\alpha$ times the initial slope of the impulse response is small. If the input is a filtered impulse, the initial part of the response will rise smoothly from zero even when the test filter has only one more pole than zero. Integral-square errors for filtered impulse inputs will also tend to remain small as $\Delta\alpha$ increases. The error scores in Table 7.5 follow this pattern.

The magnitude of the ISE caused by delay can be reduced by decreasing the sampling interval and thereby decreasing the size of the smallest increments of delay compensation. Since it is always possible to encounter a test filter whose delay lies halfway between the delay compensation increments available to the computer, the maximum delay deviation is one-half the sampling interval.

However, if mimic coefficients must be measured with filtered random inputs in the presence of remnant, it seems unavoidable that with certain types of test filters errors will be made in measuring the delay of the system. **Nevertheless, the computed delay compensation will yield the least ISE approx**imation to the response of the system or human operator that is being measured.

3. Analog Test Filter with Noise Input.

a. Conditions of Experiment.

(1) Test Filter: Analog $1/(s + 0.5)$.

(2) Mimic Filter Poles: Same as before.

(3) Input for Measurement of Coefficients: White Noise passed through filter with transfer function $1/(s + 1.5)$.

(4) Sample length: 150 seconds.

(5) Sampling interval: 0.1 second.

b. Results.

The mimic coefficients obtained by analyzing this filter are in Table 7.6. Also shown are coefficients obtained by analyzing a digital filter having the same pole. The input for the measurement of the digital filter was unfiltered digital impulsive noise.

The first three coefficients for the analog and digital filters are very nearly the same. Coefficients b_4 and b_5 are not in good agreement. However, these coefficients are small and do not contribute much to the mimic response.

In Fig. 7.5 is a Bode plot of the transfer function of the mimic of this analog filter. It agrees very closely with the true Bode plot of a filter with transfer function $1/(s + 0.5)$.

Thus, as we would expect, the measurement method, when applied to measurement of analog filters, yields results that are essentially the same as those obtained with digital test filters. The differences, small as they are, are probably due to the fact that the digital filter only approximates the analog filter.

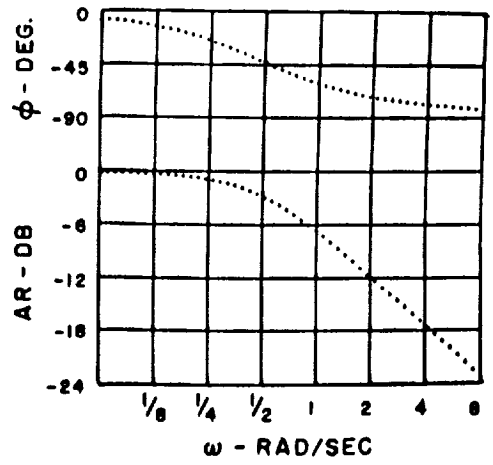

Figure 7.5.- Bode plot of analog filter 1/(s + 0.5) obtained using mimicking technique.

TABLE 7.6 - COEFFICIENTS FOR THE SAME ANALOG AND DIGITAL FILTER

TEST FILTER	b_1	b_2	b_3	b_4	b_5
DIGITAL 1/(s + .5)	.5962	.6992	.4029	.0019	.0029
ANALOG 1/(s + .5)	.5970	.7032	.4352	.0354	.0226

C. MEASUREMENT OF TIME-INVARIANT AND TIME-VARIANT HUMAN OPERATOR DYNAMICS.

The analysis programs were used to determine quasi-linear transfer functions or describing functions for human operator tracking response characteristics in a simple manual control system (described in ref. 9) The input signal to the control system was essentially white gaussian noise filtered by $1/(s + 1.5)$. The system dynamics was a simple amplifier with unity gain. The input signal had fairly large high frequency content and was moderately difficult to track. Measurements of time-variations in human operator transfer function were made by analyzing five second segments of input and operator response data. The mimic filters used in these measurements had poles at s = -1.0, -1.73, -3.0, -5.19, and -9.0. The residual error variance for the entire 150 second run was computed to be about eight percent of the operator output power.

The mimic filter pole locations were selected so as to yield small σ_{bj} (standard deviation of the mimic coefficients) and still provide a good approximation to a wide range of human operator characteristics. From measurements of the closed-loop transfer function made with the mimic filter set used to analyze the digital test filter discussed in Section VII B, it was observed that the amplitude ratio was approximately 0 db for frequencies below 1 radian per second and fell off rapidly above 4 radians per second. Thus the poles of this transfer function were likely to be in the region between 1 radian per second and 4 radians per second and perhaps higher. To make the bandwidth of the first filter large, thereby increasing M (or $2W_{ju}T$), the number of degrees of freedom in Eqs. (4.6) and (5.6), the pole of the first filter was placed at s = -1.0. This is roughly the frequency of the first significant change in amplitude ratio. The poles of the remaining were spaced equally on a logarithmic scale, the ratio of the pole positions being $\sqrt{3}$. This ratio gave a set of mimic filters whose poles were likely to span the region in which the poles of the transfer function being measured were thought to be.

In Table 7.7 are the mimic coefficients for the first 10 five second segments of the tracking run and for the entire 150 second tracking run.

TABLE 7.7 - MIMIC COEFFICIENTS FOR HUMAN OPERATOR TRACKING CHARACTERISTICS FIRST TEN 5-SECOND SEGMENTS AND ENTIRE 150 SECOND TRACKING RUN

FIVE-SECOND SEGMENT NUMBER	MIMIC COEFFICIENTS				
	b_1	b_2	b_3	b_4	b_5
1	1.11	1.05	1.29	.81	.49
2	1.14	1.20	1.32	1.26	.61
3	.98	.88	.82	.73	.52
4	.91	1.04	1.10	1.06	.45
5	.86	1.09	1.00	1.07	.43
6	.86	.84	.90	.85	.15
7	.97	1.06	1.02	.72	.46
8	.79	.48	.50	.37	.17
9	.47	.55	.59	.48	.11
10	.80	.59	.69	.50	.24
Entire Tracking Run of 150 seconds	.99	.88	.89	.65	.27

These coefficients are for the closed-loop characteristics of the control system. The delay compensation that gave least ISE was 0.1 second.

In Fig. 7.6 are Bode plots of the transfer function of the closed loop for the entire run (Fig. 7.6a) and for the second and ninth five-second segments (Fig. 7.6c and 7.6d). These transfer functions include the time delay of 0.1 second. In Fig. 7.6b are Bode plots obtained by analyzing the same data with a cross-spectrum computer built several years ago to analyze human operator tracking data (ref. 9). The agreement in the Bode plots obtained by the two methods of computation, Figs. 7.6a and 7.6b, is close. The greater scatter in the spectral analysis results is caused by the narrow bandwidth of the filters used in that analyzer. The Bode plots for the second and ninth five second segments of tracking data, Figs. 7.6c and 7.6d, show considerable difference in amplitude ratio of the transfer functions. Oscillograph records of input and response signals also show that the gain for segment 9 is much lower than segment 2. Differences between coefficients b_1, b_2, and b_3 for segments 2 and 9 were statistically significant at the 0.9 level.*

In Fig. 7.7a are plots of the power spectra of the input signal and output signal. These spectra measurements agree closely with measurements made using the cross-spectrum computer. In Fig. 7.7b is a plot of the power spectrum of the pilot's remnant. The remnant spectrum obtained with the cross-spectrum computer is plotted in Fig. 7.7c. The greater scatter in the cross-spectral measurements of remnant (Fig. 7.7c) is probably a result of the fact that the remnant spectrum was computed from Eq. (3.27) rather than from the remnant signal $\epsilon(\tau)$ as was the case for the spectrum in Fig. 7.7b.

It should be noted that these measurements of human operator dynamics are of the closed-loop transfer function and were made using the forcing function input to the system and the pilot's response. The mimicking technique offers the possibility of measuring directly pilot open-loop transfer function by using the error and response signals. This kind of measurement

---

* Differences were tested using the t test as discussed in Section IV B.

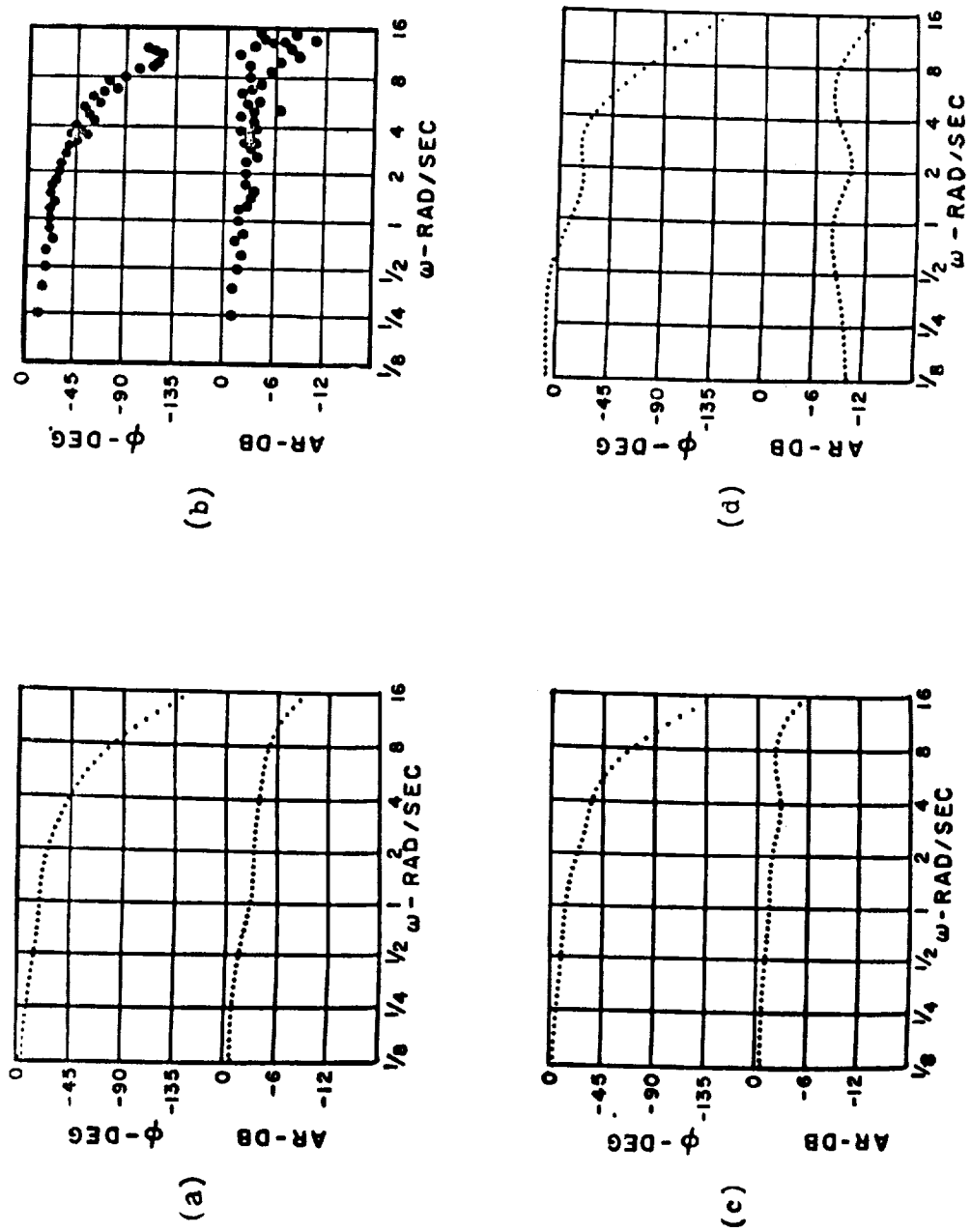

Figure 7.6.- Bode plots for closed-loop transfer functions for human pilot in simple manual control system. (a) Bode plot for entire run determined by mimicking technique. (b) Bode plot for entire run obtained by spectral analysis with cross-spectrum computer. (c) and (d) Bode plots for second and ninth 5-second segments of tracking run.

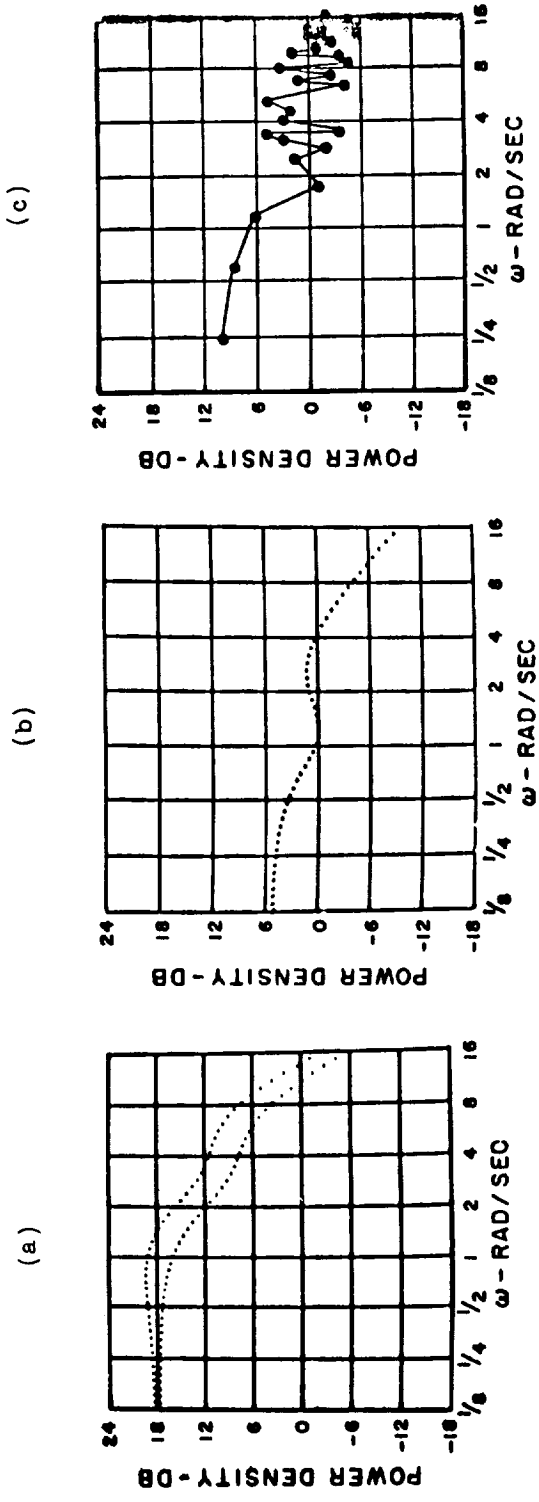

Figure 7.7.- Power spectra of pilot input and output signals (a), and of pilot remnant (b) computed using mimicking technique. Power spectrum of pilot remnant computed using cross-spectrum computer (c). The upper curve in (a) is the input spectrum and the lower curve is the output spectrum. The spectra obtained using the mimicking technique are plotted in db relative to the same arbitrary reference. The remnant spectrum obtained using spectral analysis is relative to a different reference.

is not possible with the usual cross-spectral techniques. For control situations in which appreciable error power exists beyond the effective bandwidth of the system input forcing function (such as might be observed when the pilot is controlling a lightly dampened vehicle with a natural frequency higher than the input bandwidth), the error power at these frequencies would be included in the pilot's remnant if cross-spectral methods of analysis were used. If the mimicking technique were used, this component of error would probably be accounted for in the pilot's transfer function.

We have not yet been able to determine if the pilot's transfer function determined from closed-loop measurements (using input signal) is different from that determined from open-loop measurements (using the error signal). The mimicking technique makes possible comparison of these two types of transfer function. It would seem that the open-loop measurement, since it actually takes into account all of the signal to which the pilot responds (not just the part correlated with the input), should be a more appropriate description of pilot behavior.

VIII. CONCLUSIONS

The theoretical and experimental results demonstrate that the measurement by mimicking technique is well suited to measurement of linear time-invariant and linear time-variant dynamic systems whose output is disturbed by noise. The technique has a number of advantages. The use of a mimic composed of a set of physically realizable filters insures that the system characteristics determined from the measurements will also be realizable. As a result, control system elements can be measured in situ, that is, with the signals normally circulating in the control loop and without altering the connections of the system without encountering difficulties with respect to the realizability of the measured characteristics (ref. 19). A second advantage stems from the fact that the entire covariance matrix of Eq. (3.9) is used to determine mimic coefficients, not just the diagonal terms. Therefore, it is not necessary to require that the filter outputs be orthogonal over the sample used in the measurement, as is the case in power spectral analysis method of measurement (ref. 9). Consequently, shorter samples of signals can be used than would be possible if orthogonality were necessary. Third, few restrictions are placed on the type of filters used in the mimic. By choosing filters that resemble the characteristics of the system being measured, the variance of the measurements can be reduced or, alternatively, the sample length can be reduced.

Perhaps, the most important advantage of the measurement by mimicking technique is the relative simplicity of the relations for the variance of the mimic coefficients, Eqs. (4.1) and (4.6). Sample length requirements can be estimated easily from these equations. Confidence limits for measured values of the coefficients can be made using simple statistical techniques.

The variance of the measurements of mimic coefficients determines the sample length required to find the mimic coefficients to within specified confidence limits. The variance of the mimic coefficients depends directly upon the variance of the residual, inversely upon the bandwidth of the residual, and inversely upon the variance of the part of the output of each

mimic filter output that is uncorrelated with the other filter outputs. It also depends upon the bandwidth of the uncorrelated part of the mimic filter outputs.

By choosing mimic filters carefully, the residual variance can be reduced, and the bandwidth of the mimic filter outputs can be increased. The mimic filters should be chosen so that their impulse responses resemble the impulse response of the system being measured. If this is done an accurate representation of the system can be obtained with only a few filters. Orthogonalized exponential filters having real poles are recommended for measurement of systems whose poles are also real or located close to the real axis of the complex frequency plane. A single set of five such filters with poles spaced uniformly on a logarithmic scale is capable of approximating the impulse responses of a wide variety of systems with a relative integral-square error of about one per cent or less.

In an actual measurement situation, the following procedure, which was employed in making the measurements of human operator time-varying characteristics discussed in Section VIIC, is a reasonable one to use when applying the measurement by mimicking technique. Estimate the approximate location of the poles of the system being measured. Take a relatively long sample of data and analyze it with a set of mimic filters whose poles more than span the range of the poles of the system. A good choice is a set of mimic filters whose poles are spaced uniformly on a logarithmic scale. Using the results of the measurements, choose another set of mimic filters that are better matched to the system characteristics in the sense that this second filter set resembles the system as closely as possible. Choose filters whose bandwidths are as large as possible consistent with the requirement for a good match. This second set of mimic filters will provide a better approximation to system characteristics and will yield mimic coefficients having smaller variance than the first set. It will also be better suited for determining time-varying characteristics of the system or of the human operation.

Bolt Beranek and Newman Inc.
Cambridge, Mass., July 31, 1962

APPENDIX A

IMPLEMENTATION OF ANALYSIS TECHNIQUE

A. DIGITAL IMPLEMENTATION

To carry through an analysis of human pilot dynamic characteristics, a number of different kinds of mathematical operations are required. To determine a quasi-linear transfer function for the pilot, the input signal $x(t)$ must be filtered by the mimic filters; the covariance matrix $\underline{L}$ of Eq. (3.12) must be computed; the matrix equation (3.12) must be solved for the mimic coefficients; the mimic transfer function must be determined; and the transfer function must be plotted vs. frequency. A similar set of operations is required to determine the power spectrum of the remnant.

It is desirable to perform all these operations on a single computer so that a complete analysis of pilot characteristics can be performed without resorting to hand computations and manipulations of data or intermediate results. Although the filtering operations are easily done on an analog computer, most of the other functions cannot be handled easily on such a computer. A high speed digital computer can perform the filtration and is well suited for all the other operations including preparation of plots of transfer functions.

We have used a high speed digital computer to implement and evaluate the analysis technique discussed in this report. Programs to perform the required mathematical operations have been written for the Digital Equipment Corporation's PDP-1B computer (ref. 34). It is a high speed (10 microsecond add time, for example), relatively low cost (approximately $150,000) machine that has good input-output facilities. Clearly the measurement technique can be programmed on other digital computers. It is hoped that this appendix will provide sufficient information for writing such programs. The orthonormal filtering and covariance operations are easily programmed for an analog computer (see ref. 26 for discussion of analog implementation), but the matrix operations are not easy to do on such a machine.

B. FUNCTIONAL DESCRIPTION

In Fig. A.1 is a flow diagram showing the principal operations performed by the digital computer analyzer programs. The operations are divided into three groups: Group I is Data Acquisition; Group II is Analysis; and Group III is Transformation and Display.

The Data Acquisition Group performs the tasks of (1) digitalizing the analog input and output signals, (2) compacting the digitalized signals for efficient storage of data, and (3) producing a punched paper tape containing the digitalized signals. This digital tape is then used as the input to the Analysis programs. The digitalization is performed by a commercial analog-to-digital converter.

Since two signals, input $x(t)$ and $y(t)$, must be converted, a relay commutator is used to connect the converter alternatively to the two signals. The Compacting program combines the two nearly simultaneous samples of input and output into one computer word and stores the word in memory. The Tape Preparation program punches the stored data on paper tape or writes it on magnetic tape instead of paper tape.

The Analysis Group of operations is performed in two steps. First, as shown in Group IIa of Fig. A.1, the digital data tape is read in and fed to the Delay Compensation program. This program advances pilot output $y(t)$ in time relative to the input $x(t)$. Several output signals, $y(t + \delta)$, are obtained from this program, each advanced in time a different amount. The input $x(t)$ is fed to the Analysis Filter program. This program simulates a set of orthonormal analysis filters constructed using the Kautz procedure, Eq. (6.4). The filter outputs are used by the Covariance program to compute the covariance matrix $\underline{L}$ of Eq. (3.12) and the covariance vector $\underline{y}$ of that equation. These covariances are used by the Matrix Solution program to find mimic coefficients. A set of mimic coefficients are determined for each delay compensation. The delay compensation that provides the best approximation to pilot output is identified. The Covariance program also computes the covariances $\overline{z_i x}$ of Eq. (3.19), which are the coefficients of the series

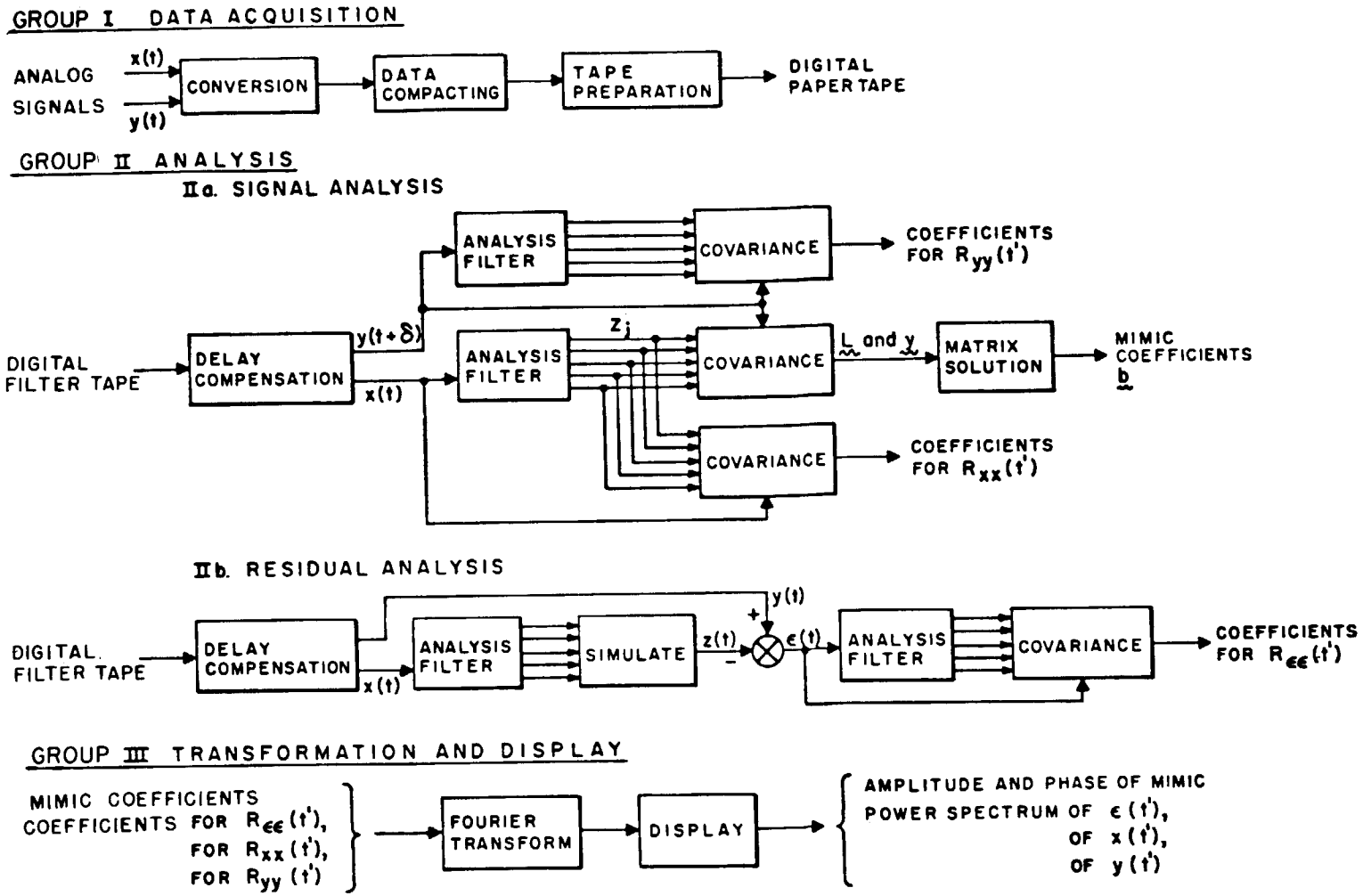

Figure A.1.- Flow diagram of digital computer implementation of analysis technique.

representation for the autocorrelation function of the input, $R_{xx}(t')$, of Eq. (3.18). The output signal y(t) is also fed to a set of analysis filters and the coefficients of the series representation of the autocorrelation function of the y(t), $R_{yy}(t')$, are determined. The variances of x(t) and y(t) are also computed by the Covariance program.

In the second part of the Analysis Group (Group IIb in Fig. A.1), the residual signal $\epsilon(t)$ and its autocorrelation function are computed. The digital data tape is read again and the input x(t) is fed to the Delay Compensation program. This program delays the input by an amount equal to the time delay that was found in the first part of the analysis to give the best approximation to pilot output. This delayed input is fed to the Analysis Filter program. The Simulate program weights each of the outputs of the Analysis Filter program by the appropriate mimic coefficient as determined in the first part of the analysis. The weighted outputs are summed to give the mimic output z(t), which is subtracted from the pilot output y(t) to yield the residual $\epsilon(t)$. The residual is fed to the Analysis Filter program and the coefficients of the series representation of the autocorrelation function of the residual, $R_{\epsilon\epsilon}(t')$, are computed from the filter outputs by the Covariance program. The variance of the residual is also computed by the Covariance program.

The Transformation and Display Group of programs (Group III in Fig. A.1), computes the transfer function of the mimic and the power-density spectra of input, output and residual. These computations require the coefficients of the mimic and the coefficients of the series representation of the input, output and residual autocorrelation functions, and are performed by the Fourier Transform program. The amplitude ratio and phase of the transfer function and the power spectra are determined at as many frequencies as desired. These are spaced uniformly on a logarithmic scale. The amplitude ratio and power spectra are converted to a decibel scale. The Display program generates a grid and then plots the amplitude ratio in db, the phase angle in degrees, and the power spectra in db against the logarithm of frequency. In this way Bode plots of the pilot's characteristics can be obtained and photographed. Paper tapes containing the numerical values of the displayed quantities can be produced if desired.

The first part of the Analysis Group of programs takes about 0.2 second per data point analyzed to perform its entire set of operations. Thus, if human operator data is sampled at the rate of ten times per second, the mimic coefficients and coefficients of the input and output spectra could be computed at twice running time. The second part of the Analysis Group requires about 0.1 second per data point. The entire Analysis Group, therefore, will take three times real time for a sampling rate of ten per second. The Transform and Display Group of programs requires about 0.7 second to compute the mimic transfer function and the three power spectra per frequency.

C. ORGANIZATION OF COMPUTER PROGRAMS

About 100 individual programs or subroutines are used to implement the analysis technique. These programs have been organized into a hierarchy of Utility and Computation subroutines, Control programs and Master programs. The Control programs perform the functions represented by the blocks of Fig. A.1. That is, the blocks labelled Analysis Filter, Covariance, Simulate, etc. each designate a Control program. The Control programs call Computation and Utility subroutines to do the arithmetical and logical operations required for the function being performed. A Master program calls the Control programs in proper sequence and designates the location of the arguments to be used by each Control program. The sequence of functions indicated by the flow diagrams of Fig. A.1 is determined by a Master program.

Control programs are always called by the Master program and always return to the Master program when they have completed the operations they perform. Computation subroutines are called by Control programs and return to the Control program. Similarly, the Utility programs return to the Control or Computation programs that called them.

A "Table of Contents" and a "Table of Arguments" are used in the programming system. The Table of Contents is an itemized list of all the programs that are in the computer and gives the beginning address of each pro-

gram. All programs are called by referring to a memory register in the Table of Contents and then transferring control to the instruction whose address is the contents of that register. That instruction is the initial instruction of the program desired. The Table of Arguments is a list of parameters and addresses of parameters that are used by Control programs. For example, the Table of Arguments contains the address of the input to be used by the Analysis Filter program at a particular stage of the analysis and the initial address of the block of memory in which the filter outputs should be deposited. Space is allotted in the Table of Arguments for each of the Control programs that can be called by the Master programs. Computation and Utility subroutines always are given the arguments they require or their locations by the Control program that calls them.

To perform a particular operation, such as Analysis Filter, the Master program specifies the initial location in the Table of Arguments of the set of arguments required by the Analysis Filter Control program. The Master program then calls the Analysis Filter Control program by specifying the address in the Table of Contents of that program. The following is a portion of the Master program that causes the digital data input to be read, the signals to be compensated for time delay, and both input and output to be filtered by the Analysis Filter program. These are the first few operations performed by the Analysis Group of Fig. A.1.

```
input 3
 law 1
delay comp
 law 1
 filter
 law 2
 filter
   ⋮
```

The instruction "input 3" causes the computer to go to the register in the Table of Contents that contains the address of the first instruction of the "input 3" program and then to execute that instruction. The "input 3" program is the program that reads the digital data tape. Since only one

set of arguments is used with that program, designation of arguments is not necessary. "law 1" and "law 2" are computer instructions that cause the numbers one (1) and two (2) to be deposited in the accumulator. These numbers designate the first and second sets of arguments for the program whose name follows the "law" instruction. The instructions "delay comp" and "filter" refer to the locations in the Table of Contents that contain the addresses of the first instructions of the Delay Compensation and of the Analysis Filter Control programs. Since two signals are to be filtered by the Analysis Filter program, two different sets of arguments must be designated. Note that "law 1" precedes the first filter instruction and "law 2" precedes the second.

Master programs are short and simple. They are easy to write or change in the event some modification in the analysis technique is required. The Table of Contents and Table of Arguments provide considerable flexibility in the use of programs. When new programs are added to the system, old programs are modified, or the locations of programs are changed, only changes or additions to the appropriate initial addresses contained in the Table of Contents are required. Since all programs are called through the Table of Contents, it is not necessary to change any of the calling sequences of existing programs or to recompile or reassemble existing programs. Changes in the arguments used by a program can be made by changing entries in the Table of Arguments or by changing the "law" instructions in the Master program so that different sets of arguments are used.

D. PROGRAM DETAILS

1. Group I - Data Acquisition.

Mercury-wetted relays under computer control are used to commutate between the input and output analog signals. Maximum commutating rates of the relays are about 200 per second, allowing a sample from the pair of signals at a rate of 100 per second. An Epsco TB 711 Transicon (ref. 37) is used as the analog-to-digital converter.

The Conversion program first switches a relay, instructs the analog-to-digital converter to take a sample, waits until the converter indicates that it has converted the sample, and then reads the output register of the converter. The relays are then switched and the converter reads the second channel as soon as possible after the first channel of data is taken. The computer waits until the computer clock indicates that it is time to take another pair of samples.

While waiting, the computer compacts the pair of samples into one word. The signals are also displayed on the cathode ray tube display of the computer and the operator is provided with a continuous monitor of both data channels. The computer will not start storing data into memory until it has been instructed to do so by the operator. At the conclusion of the data run, the data is punched onto paper tape.

With a sampling rate of ten per second, approximately 350 seconds of data can be stored in memory-when the sampling rate is ten per second. When magnetic tape storage is used, converted data can be written on the tape as rapidly as it is sampled and the size of the computer memory does not limit the length of the tracking run that could be converted.

2. Analysis Group.

a. Analysis Filter Program.

The Analysis Filter program simulates a set of orthogonalized exponential filters constructed according to the Kautz procedure, Eq. (6.4). As many filters can be contained in the set as desired. In most of our work, we have used four or five filters.

The Kautz filters have the transfer functions that can be written

$$\Phi_1(s) = \frac{\sqrt{2s_1}}{(s + s_1)}$$

$$\Phi_2(s) = \frac{\sqrt{2s_2}\ (s - s_1)}{(s + s_1)(s + s_2)} = \sqrt{\frac{s_2}{s_1}}\,\frac{(s - s_1)}{(s + s_2)}\ \Phi_1(s)$$

$$\Phi_3(s) = \sqrt{\frac{s_3}{s_2}}\,\frac{(s - s_2)}{(s + s_3}\ \Phi_2(s) \qquad \text{(A.1)}$$

$$\Phi_i(s) = \sqrt{\frac{s_i}{s_{i-1}}}\,\frac{(s - s_{i-1})}{(s + s_i)}\ \Phi_{i-1}(s)$$

The first filter is a simple first order lag. The second filter is a cascade connection of the first filter and a filter having a transfer function

$$\sqrt{\frac{s_2}{s_1}}\,\frac{(s - s_1)}{(s + s_2)} \qquad \text{(A.2)}$$

All succeeding filters can be constructed by cascading the previous filter and a filter having a transfer function of the form of Eq. (A.2).

The transfer function of Eq. (A.2) can be decomposed as follows:

$$\sqrt{\frac{s_2}{s_1}}\,\frac{(s - s_1)}{(s + s_2)} = \sqrt{\frac{s_2}{s_1}} - \sqrt{\frac{s_2}{s_1}}\,\frac{(s_2 + s_1)}{(s + s_2)} \qquad \text{(A.3)}$$

Equation (A.3) is recognized as a transmission plus a first order lag. Taking advantage of Eq. (A.3), the set of orthonormal filters of the form

of Eq. (A.1) can be synthesized from simple first order lags and simple transmissions in the manner shown in Fig. A.2.

The basic building block of the filter set is a first order lag, $1/(s + s_i)$. The impulse response of a filter of this form is

$$g_i(t) = e^{-s_i t} \tag{A.4}$$

In terms of the impulse response, the output of the filter r(t) is

$$r(t) = \int_{-\infty}^{t} c(t')\, g(t-t')\, dt'$$

or

$$r(t) = \int_{-\infty}^{t} c(t')\, e^{-s_i(t-t')}\, dt' \tag{A.5}$$

where c(t) is the input to the filter.

The digital computer has only sample values of c(t) available to it. An approximation to Eq. (A.5) is desired when these sample values are used. Assume that samples of c(t) and r(t) are taken every h seconds. The value of c(t) and r(t) at time t = nh will be designated $c(t_n)$ and $r(t_n)$.

Equation (A.5) may be written:

$$r(t_{n+1}) = \int_{-\infty}^{t_{n+1}} c(t')\, e^{-s_i(t_{n+1}-t')}\, dt' \tag{A.6}$$

since

$$t_{n+1} = t_n + h,$$

then

$$r(t_{n+1}) = e^{-s_i h} \int_{-\infty}^{t_n} c(t')\, e^{-s_i(t_n-t')}\, dt' + \int_{t}^{t_{n+1}} c(t')\, e^{-s_i(t_{n+1}-t')}\, dt' \tag{A.7}$$

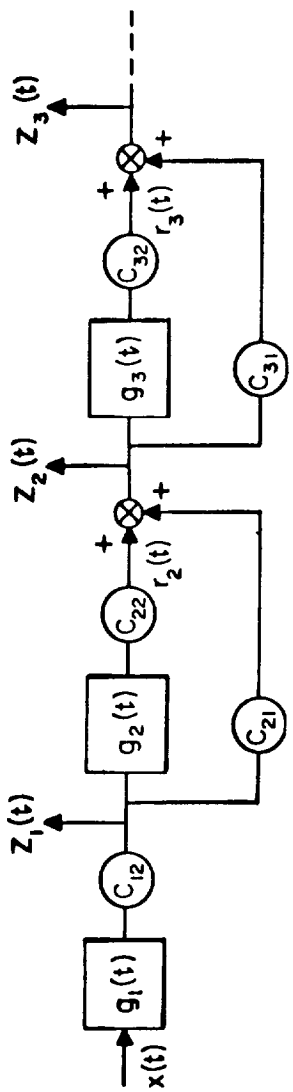

Figure A.2.- Implementation of Kautz procedure for generating set of orthonormal exponential filters.

The first integral on the right is equal to $r(t_n)$. The second integral must be approximated from values of $c(t)$ at t_n and t_{n+1}. We have used a trapezoidal rule for numerical approximation of the integral. Using this rule, we obtain

$$r(t_{n+1}) = r(t_n)\, e^{-s_i h} + \frac{h}{2}\left[c(t_{n+1}) + c(t_n)\, e^{-s_i h}\right] \qquad (A.8)$$

Thus, the value of r at t_{n+1} is related to the values of r and c at t_n and to the value of c at t_{n+1}.

By making use of Eq. (A.8), we obtain the following equation for the digital approximation to the first filter of Fig. A.2.

$$z_1(t_{n+1}) = C_{12}\frac{h}{2}\left[x(t_{n+1}) + x(t_n)\, e^{-s_1 h}\right] + z_1(t_n)\, e^{-s_1 h} \qquad (A.9)$$

The equations for the second filter are

$$z_2(t_{n+1}) = C_{21}\, z_1(t_{n+1}) + C_{22}\left[\frac{h}{2}\, z_1(t_{n+1}) + z_1(t_n)\, e^{-s_2 h}\right] + r_2(t_n)\, e^{-s_2 h} \qquad (A.10)$$

$$r_2(t_n) = C_{22}\frac{h}{2}\left[z_1(t_n) + z_1(t_{n-1})\, e^{-s_2 h}\right] + r_2(t_{n-1})\, e^{-s_2 h}$$

Succeeding filters are approximated by equations similar to Eq. (A.10). From Eq. (A.3), it may be seen that

$$C_{11} = 0$$

and

$$C_{i1} = \sqrt{s_i / s_{i-1}} \quad \text{for} \quad i \neq 1$$

$$C_{12} = \sqrt{2 s_1} \qquad (A.11)$$

$$C_{i2} = \sqrt{\frac{s_i}{s_{i-1}}}\,(s_2 + s_1) \quad \text{for } i \neq 1$$

A single exponential filter program based on Eqs. (A.9) and (A.10) is used repetitively to perform the several filtering operations indicated in Fig. A.2. The first data point of the input is applied to the filter program, producing the first output point of filter 1. This output point of filter 1 is now used as the input to filter 2, and so forth. The computation is performed point by point. The constants used by the program to simulate the set of filters diagrammed in Fig. A.2. C_{12}, C_{22}, C_{31}, etc., are computed in advance and stored in a table. These constants are used as required by the program.

The digital filter does not of course match an analog exponential filter exactly. The difference between the output of the digital filter and the corresponding analog filter depends upon the input. If the input is an impulse, the initial point of the response of the digital filter will be one-half of the correct value. All other points will equal the analog filter response.

b. Covariance Program.

The covariance of two signals is computed by using a Simpson's Rule approximation for the integral

$$\frac{1}{T} \int_0^T z_i(t)\ z_j(t)\ dt \qquad (A.12)$$

The covariances are computed point by point.

The accuracy of the Simpson's Rule approximation used in the covariance program has been evaluated by computing covariances of known functions. The approximation is satisfactory for the kind of analysis being performed. For example, when the covariance program is used to find the integral square of the impulse response of a simple exponential filter, the computed values are within 0.5 per cent of the correct values when the sampling interval h is between .02 and .5 times the filter time constant (ref. 36). Actually, most of this error results from the trapezoidal approximation used in the Analysis Filter program rather than from approximations in the Covariance program, When the Covariance program is used to find the integral square of the exact exponential function

$$r(t_n) = e^{-.5nh} \qquad (A.13)$$

a value of 0.999862 is obtained. This differs by .0138 per cent from unity,

the value of the integral square of the corresponding continuous function (ref. 37)

$$r(t) = e^{-.5t} \tag{A.14}$$

c. Matrix Solution.

The set of equations, Eq.(3.9), is solved by a simple iterative technique. The first equation is solved for b_1 by setting all other coefficients to zero. This value of b_1 is used to find b_2 in the second equation when all higher order coefficients are equal to zero. Initial values of the remaining coefficients are found by continuing this process. The initial values for all coefficients except b_1 are then substituted into the first equation, and a new value for b_1 is obtained. This value is used in the second equation to find b_2. The process is continued until the fifteen most significant binary digits of all coefficients remain unchanged after two successive iterations.

After the mimic coefficients are computed, the program computes the integral square of the residual error. Equation (3.26) is used to obtain the residual integral square from the covariances s_y^2 and $\overline{z_1 y}$. When the residual error is very small, this method of computing the residual integral square will be inaccurate because the computation involves subtraction of large numbers whose differences are small.

3. Transformation and Display Group.

a. Fourier Transform Program.

This program first computes the real and imaginary parts of the Fourier transforms of the orthonormal filter impulse responses used in the Analysis Filter program. These transforms are the transfer functions of the filters. The program then uses these transfer functions to find the mimic transfer function and the power spectra of the input, output and residual signals. All of these computations are performed for each frequency.

The transfer function of the digital low-pass filter that forms the basis of Fig. A.2 can be computed by taking the z-transform of Eq. (A.8).

The relation

$$R_{n+1}(z) = z\, R_n(z) \tag{A.15}$$

is used to relate the z-transform of $r(t_{n+1})$ and $r(t_n)$ (ref. 38). The z-transform of Eq. (A.8) can be written

$$\frac{R_n(z)}{C_n(z)} = \frac{h}{2}\left[\frac{1 + z^{-1}\, e^{-s_i h}}{1 - z^{-1}\, e^{-s_i h}}\right] \tag{A.16}$$

This is an exact expression for the digital filter. It can be converted to frequency domain by noting that

$$z = e^{j\omega h} \tag{A.17}$$

Making this substitution, we obtain for the transfer function of the filter of Eq. (A.8)

$$G_i(j\omega) = \frac{R_n(j\omega)}{C_n(j\omega)} = \frac{h}{2}\left[\frac{1 + e^{-j\omega h}\, e^{-s_i h}}{1 - e^{-j\omega h}\, e^{-s_i h}}\right] \tag{A.18}$$

where $R_n(j\omega)$ and $C_n(j\omega)$ are the Fourier transforms of the sampled versions of the signals $r(t)$ and $c(t)$.

The transfer functions of the mimic filters of Fig. A.2 can be obtained by proceeding in the same way. For example,

$$\Phi_i(j\omega) = \Phi_{i-1}(j\omega)\left[C_{i1} + C_{i2}\,\frac{h}{2}\,\frac{(1 + e^{-j\omega h}\, e^{-s_i h})}{(1 - e^{-j\omega h}\, e^{-s_i h})}\right] \tag{A.19}$$

b. Display Program.

The display device is a cathode ray oscilloscope controlled by the computer. Individual points of a matrix of 1024 by 1024 points can be displayed. As a part of this analyzer, the digital oscilloscope is used to display portions of the input, output, mimic, or remnant signals as a function of time. It is also used to display the Bode plots of the system or pilots being analyzed and plots of the power spectra of the signals in the system. Coordinate grids are also displayed for these plots.

REFERENCES

1. James, H.M., Nichols, N.B., and Phillips, R.S., Theory of Servo-mechanisms, McGraw Hill, New York, 1947.

2. Weiss, H.K., "Recommended Tracking Ratios for T36 Director," Memo to President Antiaircraft Artillery Board, September 1943.

3. Weiss, H.K., "Improvement of Tracking with Disturbed Reticle Sights," Memo to President Antiaircraft Artillery Board, Fort Bliss, Texas, 1945.

4. Tustin, A., "An Investigation of the Operator's Response in Manual Control of a Power Driven Gun," C. S. Memorandum No. 169, Metropolitan-Vickers Electrical Co. Ltd., Attercliffe Common Works, Sheffield, England, August 22, 1944.

5. Tustin, A., "The Choice of Response Characteristics for Controllers for Power Driven Guns," C.S. Memorandum No. 184, Metropolitan-Vickers Electrical Co. Ltd., Attercliffe Common Works, Sheffield, England, October 10, 1944.

6. Tustin, A., "The Nature of the Operator's Response in Manual Control and Its Implications for Controller Design," J. of the I.E.E., Vol. 94, Part IIA, No. 2, 1947.

7. McRuer, D.T., and E.S. Krendel, "Dynamic Response of Human Operators," WADC-TR-56-524, Wright Air Development Center, Wright-Patterson Air Force Base, Ohio, October 1957.

8. Licklider, J.C.R., "Quasi-linear Operator Models in the Study of Manual Tracking," Developments in Mathematical Psychology ed. by R.D.Luce, Glencoe, Illinois: The Free Press, 1960.

9. Elkind, J.I., and C.D. Forgie, "Characteristics of the Human Operator in Simple Manual Control Systems," IRE Trans. on Automatic Control, Vol. AC-4, pp. 44-55, May 1959.

10. Russell, L., "Characteristics of the Human as a Linear Servo-Element," M.S. Thesis, Elect. Eng. Dept. Mass. Inst. of Tech., Cambridge, Massachusetts, May 1951.

11. Hall, I.A.M., "Effects of Controlled Element on the Human Operator," Aeronautical Engineering Lab. Rept. 389; Princeton University, Princeton, New Jersey, 1957.

12. Sheridan, T.B., "Time-Variable Dynamics of Human Operator Systems," AFCRC-TN-60-169, Air Force Cambridge Research Center, Bedford, Massachusetts.

13. Huggins, W.H., "Experimental Determination of Transfer Functions for Human Operators and Machines," unpublished memorandum, Air Force Cambridge Research Center, Cambridge,Massachusetts, October 1949.

14. Wiener, N., Extrapolation, Interpolation and Smoothing of Stationary Time Series, John Wiley and Sons, New York, 1950.

15. Lee, Y.W., Statistical Theory of Communication, John Wiley and Sons, New York, 1960.

16. Elkind, J.I., "Tracking Response Characteristics of the Human Operator," M.S. Thesis, Elect. Eng. Dept., Mass. Inst. of Tech., Cambridge, Massachusetts, May 1952.

17. "Investigation of Control Feel Effects on the Dynamics of a Piloted Aircraft System," Goodyear Aircraft Corp. Report GER 6726, April 1955.

18. Ornstein, G.N., "Applications of a Technique for the Automatic Analog Determination of Human Response Equation Parameters," Report No. NA61H-1, North American Aviation, Inc., Columbus, Ohio, January 1961.

19. Goodman, T.P. and J.S. Reswick, "Determination of system Characteristics from Normal Operating Records," Trans. ASME, February 1956.

20. Levin, M.J., "Optimum Estimation of Impulse Response in the Presence of Noise," IRE Trans. on Circuit Theory, Vol. CT-6, pp. 50-56, March 1960.

21. Cramer, H., Mathematical Methods of Statistics, Princeton University Press, Princeton, New Jersey, 1951.

22. Hald, A., Statistical Theory with Engineering Applications, John Wiley and Sons, New York, 1952.

23. Levinson, N.L., "The Wiener RMS Error Criterion in Filter Design and Prediction," Appendix to Extrapolation, Interpolation and Smoothing of Stationary Time Series, by N. Wiener, John Wiley and Sons, New York, 1950.

24. Gabor, D., W.P.L. Wilby, R. Woodcock, "A Self-Optimizing Non-Linear Filter, Predictor, and Simulator," Information Theory, C. Cherry (editor), Butterworth's, London, 1961.

25. Knowles, W.B., et al. "A Correlation Analysis of Tracking Behavior," Psychometrika, Vol. 22, No. 3, pp. 275-287, September 1957.

26. Huggins, W.H., "Representation and Analysis of Signals, Part I: The Use of Orthogonalized Exponentials," AFCRC TR 57-357, Air Force Cambridge Research Center, Bedford, Massachusetts, September 1957.

27. Kautz, W.H., "Transient Synthesis in the Time Domain," IRE Trans. on Circuit Theory, Vol. CT-1, pp. 29-39, September 1954.

28. Laning, J.H., and R.H. Battin, Random Processes in Automatic Control, McGraw-Hill, New York, 1956.

29. Lampard, D.G., "A New Method for Determining Correlation Functions of Stationary Time Series," Proc. I.E.E., Vol. 102, Part C, pp. 35-41, 1955.

30. Shannon, C.E., and W. Weaver, The Mathematical Theory of Communication, University of Illinois Press, Urbana, Illinois, 1949.

31. Davenport, W.B., Jr., Johnson, R.A., and D. Middleton, "Statistical Errors in Measurements on Random Time Funtions," J. of Applied Physics, Vol. 23, No. 4, pp. 377-388, April 1952.

32. Booton, R.C., "An Optiminzation Theory for Time-Varying Linear Systems with Non-Stationary Statistical Inputs," Proc. IRE, Vol. 40, pp. 977-981, August 1952.

33. Elkind, J.I., and D.M. Green, "Measurement of Time-Varying and Nonlinear Dynamic Characteristics of Human Pilots," ASD-TR-61-225, Aeronautical Systems Division, Wright-Patterson Air Force Base, Ohio, May 1961.

34. "Programmed Data Processor-1," Digital Equipment Corporation, Maynard, Massachusetts, 1961.

35. "Preliminary Instruction Manual, Transicon Datrac Voltage-Digital Converter," Epsco, Inc., Cambridge, Massachusetts.

36. "Quarterly Progress Report No. 3, Experimental Study and Development of Analysis Techniques for Human Operator Dynamic Characteristics," Contract NASw-185, Bolt Beranek and Newman, Cambridge, Massachusetts, March 1961.

37. "Quarterly Progress Report No. 2, Experimental Study and Development of Analysis Techniques for Human Operator Dynamic Characteristics," Contract NASw-185, Bolt Beranek and Newman, Cambridge, Massachusetts, January 1961.

38. Ragazzini, J.R., and G.F. Franklin, Sampled Data Control Systems, McGraw-Hill, New York 1958.